

Sub  
3AA

3 1176 00149 1563

~~CONFIDENTIAL~~  
UNCLASSIFIED

Copy 22  
RM L52L26

ADVANCE COPY  
DEC 23 1952

Destroyed :  
1(18)-4(21) 9-13-53

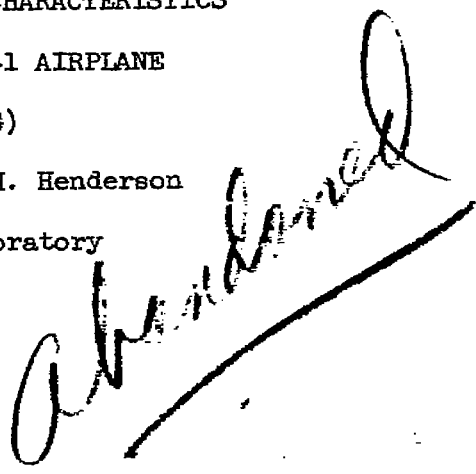
~~NACA~~ FOR REFERENCE  
NOT TO BE TAKEN FROM THIS ROOM

# RESEARCH MEMORANDUM

~~LANGLEY SUB LIBRARY~~

AN INVESTIGATION OF THE EFFECTS OF A VORTEX-GENERATOR  
CONFIGURATION ON THE AERODYNAMIC CHARACTERISTICS  
OF A 1/4-SCALE MODEL OF THE X-1 AIRPLANE  
(10-PERCENT-THICK WING)

By Jack F. Runckel and James H. Henderson  
Langley Aeronautical Laboratory  
Langley Field, Va.



**CLASSIFICATION CHANGED  
TO: UNCLASSIFIED  
PER AUTH. OF NASA HDQ. MEMO  
BYD 9-21-71, s. H. G. Maines,  
by C. E. J. 37-72**

CLASSIFIED DOCUMENT

This material contains information affecting the National Defense of the United States within the meaning of the espionage laws, Title 18, U.S.C., Secs. 793 and 794, the transmission or revelation of which in any manner to an unauthorized person is prohibited by law.

## NATIONAL ADVISORY COMMITTEE FOR AERONAUTICS

WASHINGTON

NACA LIBRARY  
LANGLEY AERONAUTICAL LABORATORY  
Langley Field, Va.

~~CONFIDENTIAL~~  
UNCLASSIFIED

UNCLASSIFIED

NACA RM L52L26

~~CONFIDENTIAL~~

NATIONAL ADVISORY COMMITTEE FOR AERONAUTICS

RESEARCH MEMORANDUM

AN INVESTIGATION OF THE EFFECTS OF A VORTEX-GENERATOR  
CONFIGURATION ON THE AERODYNAMIC CHARACTERISTICS  
OF A 1/4-SCALE MODEL OF THE X-1 AIRPLANE  
(10-PERCENT-THICK WING)

By Jack F. Runckel and James H. Henderson

SUMMARY

An investigation of a vortex-generator configuration on the wings of a 1/4-scale model of the X-1 airplane having a 10-percent-thick wing was conducted in the Langley 16-foot transonic tunnel. The effect of the vortex generators was determined by comparing the model aerodynamic characteristics, wing-pressure distributions, and wing-wake patterns for model configurations with and without vortex generators on the wings. Results are presented from tests at 0.1 increments in Mach number from about 0.69 to 0.99, at Reynolds numbers of about  $4.1 \times 10^6$  to  $4.7 \times 10^6$ , and through an angle-of-attack range up to  $15^\circ$  at lower speeds and up to  $5^\circ$  at the highest speed. In general, little difference in the aerodynamic characteristics was observed, except at a Mach number of 0.90 where a rearward movement of the shock on the upper surface of the wing with the vortex generators installed resulted in less separation.

INTRODUCTION

The use of vortex generators on the wings of airplanes has been proposed as a means of alleviating such undesirable characteristics as buffeting, lateral unsteadiness, and changes in trim resulting from flow separation. Donaldson (ref. 1) demonstrated that these devices were effective in reducing separation due to shock and boundary-layer interaction on an airfoil section. Flight tests on two unswept-wing airplanes (refs. 2 and 3) revealed that separation due to shock was delayed to higher Mach numbers or lift coefficients by the use of vortex generators. The phenomenon of buffeting has also been shown to be closely related to shock-induced separated flow over the wing and has been alleviated in some cases with vortex generators (refs. 3 and 4).

~~CONFIDENTIAL~~

UNCLASSIFIED

CLASSIFICATION CHANGED  
TO: UNCLASSIFIED  
PER AUTH. OF NASA HDQ. MEMO  
D-19 9-21-71, H. G. Maines,  
by *[Signature]* 3-1-72

As part of an investigation of a 1/4-scale model of the X-1 airplane with a 10-percent-thick wing in the Langley 16-foot transonic tunnel, vortex generators were tested to determine their effect on the model aerodynamic and fluctuating-pressure characteristics. The results of the fluctuating-pressure measurements with and without vortex generators on the wings have been reported in reference 5.

The purpose of the present report is to evaluate the effect of the vortex generators on the model aerodynamic characteristics as determined by wing-pressure distributions, wake measurements, and model force and moment measurements obtained in the wind tunnel.

Tests were run through a Mach number range from about 0.69 to 0.99 at Reynolds numbers from about  $4.1 \times 10^6$  to  $4.7 \times 10^6$  and through an angle-of-attack range up to  $15^\circ$  at lower speeds and up to  $5^\circ$  at the highest speed.

#### SYMBOLS

M	Mach number
R	Reynolds number, based on a mean aerodynamic chord of 1.203 ft
p	static pressure in undisturbed stream, lb/sq ft
$p_u$	local static pressure on upper surface, lb/sq ft
$p_l$	local static pressure on lower surface, lb/sq ft
q	incompressible dynamic pressure, lb/sq ft
P	pressure coefficient, $\frac{p_u - p}{q}$ or $\frac{p_l - p}{q}$
$P_{cr}$	pressure coefficient for local sonic velocity
H	total pressure in undisturbed stream, lb/sq ft
$H_w$	total pressure in wake, lb/sq ft.
$\Delta H$	loss in total pressure, $H - H_w$ , lb/sq ft
S	wing area, including area enclosed by fuselage, 8.116 sq ft

- $S'$  area of wing panels outboard of station A, 6.211 sq ft  
 $b$  wing span, 7.0 ft  
 $b'$  twice spanwise distance from station A to tip, 5.708 ft  
 $c$  local wing chord parallel to plane of symmetry, ft  
 $\bar{c}$  average chord of test panel  $S'/b'$ , ft  
 $c'$  mean aerodynamic chord of wing,  $\frac{2}{3} \int_0^{b/2} c^2 dy$ , 1.203 ft  
 $x$  chordwise distance from leading edge of local chord, ft  
 $y$  spanwise distance from model center line, ft  
 $y'$  spanwise distance outboard of station A, ft  
 $z$  normal coordinate referenced to chord line at  $\frac{2y}{b} = 0.274$ ,  
 positive direction upward, ft  
 $c_n$  section normal-force coefficient,  $\int_0^1 (p_l - p_u) d \frac{x}{c}$   
 $c_{m_c}/4$  section pitching moment about 0.25 local chord,  
 $\int_0^1 (p_u - p_l) \left( \frac{x}{c} - 0.25 \right) d \frac{x}{c}$   
 $C_{N'}$  wing-panel normal-force coefficient,  $\int_0^1 c_n \frac{c}{c'} d \frac{2y'}{b'}$   
 $C_L$  model lift coefficient,  $\frac{\text{Lift}}{qS}$   
 $C_D$  model drag coefficient,  $\frac{\text{Drag}}{qS}$   
 $C_m$  model pitching-moment coefficient,  
 $\frac{\text{Pitching moment about } 0.25c'}{qSc'}$   
 $\alpha$  angle of attack of fuselage center line, deg

## MODEL AND APPARATUS

The 1/4-scale model of the X-1 airplane having a 10-percent-thick wing used in this investigation has been described in reference 6. The drawings, figure 1, show the principal dimensions of the model as tested in the Langley 16-foot transonic tunnel. Photographs of the model and sting support system are presented in figure 2. The model wing, which incorporated an NACA 65-110 airfoil, had an aspect ratio of 6 and a taper ratio of 0.50, with the 0.40-chord line being unswept. The wing had an incidence angle with respect to the fuselage axis of  $2.5^\circ$  at the root and  $1.5^\circ$  at the tip.

The vortex generators used in this investigation consisted of 1/8-inch-square flat steel plates approximately 12 percent thick with rounded leading and trailing edges. The plates were set alternately at positive and negative angles of  $7\frac{1}{2}^\circ$  to the air stream to give an included angle of  $15^\circ$ , thus forming counterrotating vortices from adjacent generators. The generators were spaced 0.40 inch center to center in a spanwise direction and extended over the entire span of both wings (fig. 3(a)). The vortex generators were machined as part of a steel strip which fitted in a groove centered on the 27.5-percent-chord station of the wing.

Model forces and moments were measured with a six-component strain-gage balance mounted inside the fuselage. Pressure distributions were determined from measurements at six spanwise stations on the left wing by the method described in reference 6. Figure 1(b) presents the spanwise and chordwise location of the measuring orifices for the six spanwise stations. A few wake measurements were obtained from a rake mounted on the right side of the fuselage 0.42 chord lengths behind the wing trailing edge and at the 27.4-percent-semispan station. The rake may be seen mounted on the model in figure 3(b).

## TESTS

Force and wing-pressure data were obtained at 0.1 increments in Mach number from 0.69 to 0.99. Wake-rake data were obtained at Mach numbers of about 0.70, 0.80, 0.85, and 1.00. The Reynolds number and Mach number field for the present investigation is shown in figure 4. The angle-of-attack range was limited at high angles by loads imposed on the sting support system and varied from about  $-4^\circ$  to  $15^\circ$  at  $M = 0.69$ , and from  $-2^\circ$  to  $5^\circ$  at the maximum Mach number of this investigation. Maximum lift was obtained only for Mach numbers of 0.69 and 0.79. The data presented in this paper are for the complete model with the stabilizer incidence and elevator deflection both at  $0^\circ$ .

### ACCURACY OF MEASUREMENTS

The discussion of the accuracy of measurement of pressure coefficient, tunnel Mach number, and model angle of attack included in reference 6 applies to the data of this paper. The accuracy of the measured force and moment coefficients, based on balance accuracy and repeatability of the data is believed to be within the following limits:

$C_L$ . . . . .	$\pm 0.01$
$C_D$ . . . . .	$\pm 0.002$
$C_m$ . . . . .	$\pm 0.01$

No adjustments for sting interference or model base pressures have been applied to the aerodynamic forces and moments.

### RESULTS AND DISCUSSION

The results of the vortex-generator investigation are presented in the following figures and table:

Force measurements . . . . .	Figures 5, 6
Chordwise-pressure-distribution comparisons . . . . .	Figures 7 to 10
Spanwise-loading comparisons . . . . .	Figure 11
Wake measurements . . . . .	Figure 12
Summary of wing section and panel data . . . . .	Table 1

#### Force Data

The effects of the vortex generators on the over-all model aerodynamic characteristics are shown by the force measurement results given in figures 5 and 6. In general, there is little difference in the lift curves except at a Mach number of 0.90 where higher lift coefficients at the same angles of attack were obtained for the configuration with vortex generators (fig. 5(a)). The vortex generators had no appreciable effect on the lift-curve slopes nor were the values of maximum lift changed at Mach numbers of 0.69 and 0.79.

The drag polars (fig. 5(b)) show that in the lower-lift-coefficient range the drag coefficients were generally higher for the configuration with vortex generators. Since there is little separation at low-lift coefficients, the vortex generators were not expected to reduce drag in this region. In the low-lift-coefficient range as the speed is increased, the thinner boundary layers permit the vortex generators to extend into

the free stream, thereby resulting in higher profile drags. At the higher lift coefficients the drag coefficients obtained with the vortex generators on the wings tend to be the same or somewhat less than those for the basic wing configuration. In the case where the drag coefficients are lower with the vortex generators, the separation has been reduced by the mixing action of these devices on the boundary layer.

The pitching-moment-coefficient curves presented in figure 5(c) show that more negative pitching-moment-coefficient values were obtained at a Mach number of 0.90 with the vortex generators installed on the wings. In general, the stability of the two configurations, as indicated by these curves, was about the same. However, at a Mach number of 0.90, the instability which was present with the clean-wing configuration near zero lift has been reduced by the vortex generators, even though the model became slightly unstable up to a lift coefficient of about 0.3.

The trends of the force-measurement results with Mach number for the two configurations are shown in figure 6. The lift curves indicate that the vortex generators have a beneficial effect at a Mach number of 0.90 (fig. 5(a)) as the higher lifts obtained with these devices help to alleviate the rapid lift variation in this speed range. The vortex generators are responsible for this increase in lift since they cause a reduction in shock-induced separation on the upper surface of the wing at this speed. The drag curves indicate that, for this vortex-generator configuration, some drag penalty exists over most of the test speed range for the lift coefficients shown.

#### Wing-Pressure-Distribution Measurements

Some representative pressure distributions obtained with the vortex-generator configuration are compared with those obtained with the clean wing in figures 7 to 10. The vertical dashed line in the figures indicates the position of the vortex generators.

Chordwise-pressure-distribution diagrams at three spanwise stations obtained at a Mach number of 0.69 for two angles of attack (fig. 7) reveal that the vortex generators have practically no effect on the pressure distributions, except at the lower angle of attack, where a local disturbance (a compression followed by an expansion) exists on the upper surface covering about 0.10 chord at the location of the vortex generators. Integrated section normal-force and pitching-moment coefficients for the two configurations were about the same at all stations. The close agreement of the wing-pressure data for both configurations would be expected since the force data of figure 5 indicated close agreement at a Mach number of 0.69.



Pressure distributions obtained at all six spanwise stations are presented in figure 8 for a Mach number of 0.79 and an angle of attack of about  $4^\circ$ . Somewhat less separation exists behind the shock for the vortex-generator configuration at station D. A more rearward shock position is indicated at some of the stations for the vortex-generator configuration. Station F exhibits a more pronounced local disturbance at the position of the vortex generators than the inboard stations. This was found to be true for the tip station at all speeds and attitudes tested.

Since the force data (figs. 5 and 6) showed that the most pronounced effect of the vortex generators on the model aerodynamic characteristics occurred at a Mach number of 0.90, a more extensive presentation of the wing-pressure-distribution data for this Mach number is given in figure 9. Chordwise pressure distributions are presented only for stations A, B, and E because of a lack of manometer data at the midspan stations. At a negative angle of attack of about  $4^\circ$  (fig. 9(a)), the lower-surface pressure distributions are about the same at all stations for the configurations with and without the vortex generators. The upper-surface pressure plot reveals a local disturbance at the position of the vortex generators, previously noted for other Mach numbers, and a farther rearward position of the shock on this surface. The pressure plots for the positive angles of attack (figs. 9(b), (c), (d), and (e)) show similar rearward shock movements due to the vortex generators. As the angle of attack is increased at this Mach number, the shock on the upper surface travels forward from about 80 percent chord at angle of attack of approximately  $-4^\circ$  to about the 60-percent-chord position at an angle of attack of approximately  $7^\circ$  on the clean-wing configuration. The upper-surface shock travels forward about the same amount (20 percent of the chord) for the change in angle of attack from approximately  $-4^\circ$  to  $7^\circ$  with the vortex generators on the wings, but it remains about 10 percent of the chord farther rearward for corresponding angles of attack. This farther rearward position of the shock on the upper surface results in a smaller separated flow region, higher lifts, and greater negative pitching moments for the wing. Although the pressure distributions for the wing with the vortex generators installed were obtained at a slightly higher Mach number than those for the clean wing, which may also cause some rearward shift in the shock position, this difference in Mach number would only account for a shock travel of about 2 percent of the chord (see refs. 7 and 8). The effect of the vortex generators on the shock location shown in figure 9 is similar to results obtained in flight with an unswept-wing airplane having the same airfoil section (ref. 3). A larger difference in the shock position between the configurations with and without vortex generators was obtained in the flight tests which may have been due to the stronger induced vortices on the airplane wing ( $15^\circ$  angle of attack of each vortex generator).

The beneficial effect indicated at a Mach number of about 0.79 and that just presented at a Mach number of approximately 0.90 are not present at the highest test speed, a Mach number near 1.00 (fig. 10). Near sonic speeds the shocks for the upper and lower surfaces are at the trailing edge of the airfoil for both configurations and there are no appreciable differences in the pressure distributions.

The chordwise pressure distributions have generally indicated a local disturbance at the position of the vortex generators at all stations for the lower angles of attack and that the disturbance occurred only at the wing-tip station for the higher attitudes. The possibility of the vortex generators being completely submerged within the boundary layer at high angles of attack may account for the absence of the local disturbance in the pressure distributions; however, no measurements of the wing boundary-layer thickness were obtained in this investigation to substantiate this ratiocination. It was found that this disturbance was usually evident when the local Mach number based on the pressure coefficients in the vicinity of the vortex generators was less than about 1.2. For local Mach numbers greater than about 1.3, no disturbances occurred. At the tip station F, the local Mach number in the vicinity of the vortex generators did not exceed 1.3 for these tests. Another possible cause for the occurrence of the local disturbance at the tip station F at all angles of attack might be due to closer proximity of the pressure orifices to the vortex generator at this station. (See fig. 1(b).)

#### Spanwise Loadings

In order to show the effect of vortex generators on the wing loading, spanwise distributions are presented in figure 11 for a Mach number of 0.90 at several angles of attack. At this speed, the loading is higher at all stations on the wing for the vortex-generator configuration at all angles of attack. The distribution of the loading spanwise is somewhat different for the two configurations, however, with stations A and E generally carrying a proportionally greater load with the vortex generators on the wing. At other Mach numbers the differences in the span loadings for the two configurations were quite small as would be expected from the close agreement of the pressure distributions (figs. 7, 8, and 10). The section normal-force coefficients used in the load parameters in figure 11 are given in table I together with the normal-force coefficients for the wing panel.

#### Wake Measurements

The vortex generators were intended to reduce the separation (see refs. 1 and 2), and a wake rake was attached to the fuselage (fig. 3(b))



to measure qualitatively the wake width and intensity at one spanwise position. The present configuration of vortex generators did not reduce the local wake drag at the speeds tested as is evident from the comparisons shown in figure 12. There is little difference in the two wake patterns at a Mach number of 0.70. At a Mach number of 0.80 higher local wake losses occur for the vortex-generator configuration; at  $M = 0.85$  the wake patterns are similar for both configurations. At sonic speeds (fig. 12(d)) both the wake width and magnitude of the loss are much greater for the vortex-generator configuration. The trend of the wake patterns obtained at Mach numbers of 0.70, 0.80, and 0.85 indicates that the wake losses might have been actually less for the vortex-generator configuration at a Mach number of 0.90 as would be expected from the pressure distributions (see fig. 9(d)). Unfortunately, however, no test data which could confirm this possibility were obtained at this speed due to a curtailment of the test program.

#### CONCLUDING REMARKS

The vortex-generator installation tested in the present study was a single configuration. A more complete investigation of configurations consisting of various chordwise and spanwise positions, higher vane angles to produce stronger vortices, and various inboard alterations would be necessary to determine the most desirable combination for the wing used in these tests. The speed range where the vortex generators were effective in reducing separation cannot be exactly defined from the present tests, but the results indicate that the effectiveness of vortex generators in increasing lift may be limited to a rather narrow Mach number range in the region of adverse lift characteristics. This region for the present wing with NACA 65-110 airfoil sections occurred around a Mach number of 0.90 where the use of vortex generators resulted in higher lifts by causing a rearward shift in the position of the shock on the upper surface of the airfoil. Generally, higher drags occurred over most of the speed range with the vortex generators installed on



the wing. The limited wake measurements indicated that, over most of the speed range, higher wake losses would occur with the vortex generators on the wing.

Langley Aeronautical Laboratory,  
National Advisory Committee for Aeronautics,  
Langley Field, Va.

*Jack F. Runckel*  
Jack F. Runckel  
Aeronautical Research Scientist

*James H. Henderson*  
James H. Henderson  
Aeronautical Research Scientist

Approved:

*Eugene C. Draley*  
Eugene C. Draley  
Chief of Full Scale Research Division

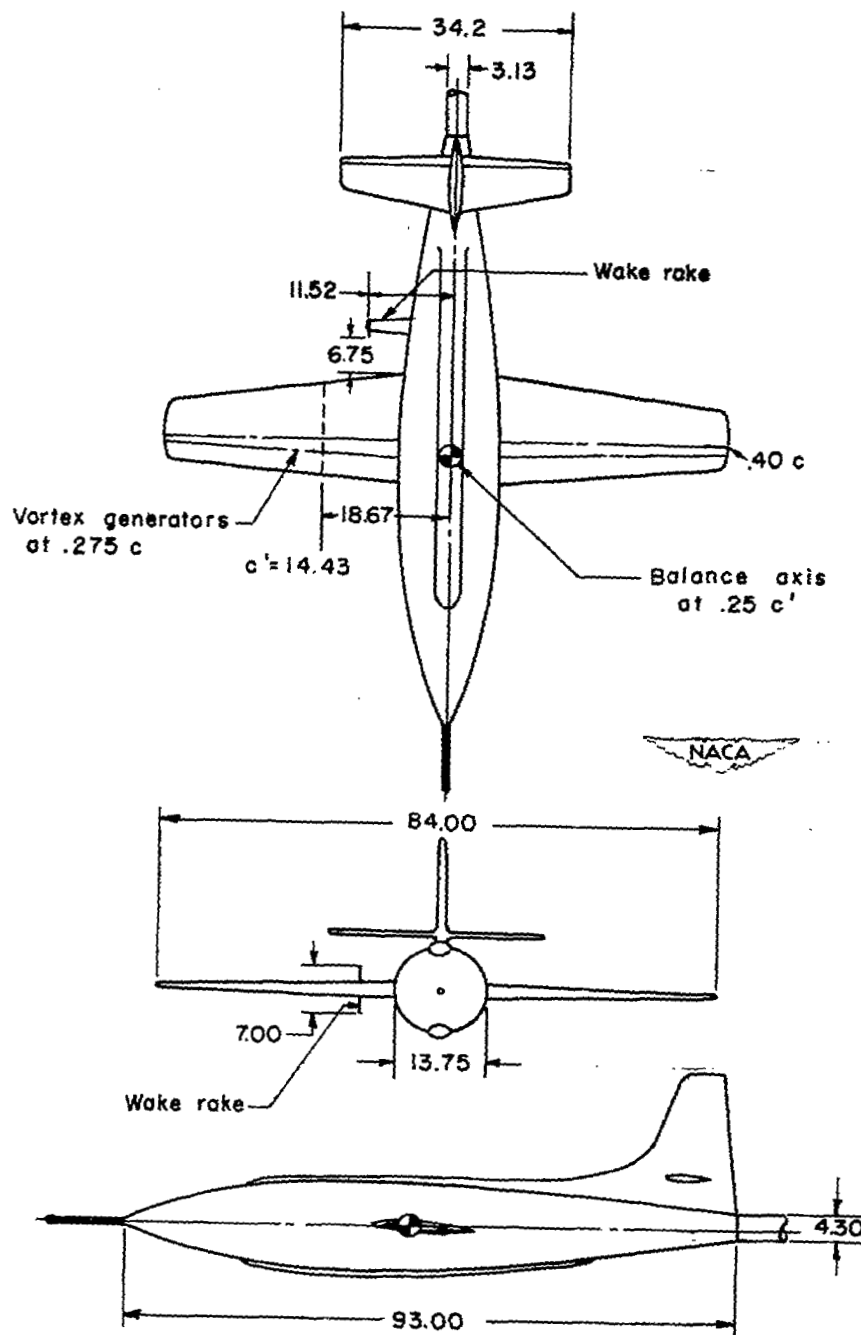
ecc

## REFERENCES

1. Donaldson, Coleman duP.: Investigation of a Simple Device for Preventing Separation Due to Shock and Boundary-Layer Interaction. NACA RM L50B02a, 1950.
2. Lina, Lindsay J., and Reed, Wilmer H., III: A Preliminary Flight Investigation of the Effects of Vortex Generators on Separation Due to Shock. NACA RM L50J02, 1950.
3. Beeler, De E., Bellman, Donald R., and Griffith, John H.: Flight Determination of the Effects of Wing Vortex Generators on the Aerodynamic Characteristics of the Douglas D-558-I Airplane. NACA RM L51A23, 1951.
4. McFadden, Norman M., Rathert, George A., Jr., and Bray, Richard S.: The Effectiveness of Wing Vortex Generators in Improving the Maneuvering Characteristics of a Swept-Wing Airplane at Transonic Speeds. NACA RM A51J18, 1952.
5. Habel, Louis W., and Steinberg, Seymour: Measurements of Fluctuating Pressures on a 1/4-Scale Model of the X-1 Airplane With a 10-Percent-Thick Wing in the Langley 16-Foot Transonic Tunnel. NACA RM L52J31, 1952.
6. Runckel, Jack F., and Henderson, James H.: A Correlation With Flight Tests of Results Obtained From the Measurement of Wing Pressure Distributions on a 1/4-Scale Model of the X-1 Airplane (10-Percent-Thick Wing). NACA RM L52E29, 1952.
7. Carner, H. Arthur, and Knapp, Ronald J.: Flight Measurements of the Pressure Distribution of the Wing of the X-1 Airplane (10-Percent-Thick Wing) Over a Chordwise Station Near Midspan, in Level Flight at Mach Numbers From 0.79 to 1.00 and in a Pull-Up at a Mach Number of 0.96. NACA RM L50H04, 1950.
8. Beeler, De E., McLaughlin, Milton D., and Clift, Dorothy C.: Measurements of the Chordwise Pressure Distributions Over the Wing of the XS-1 Research Airplane in Flight. NACA RM L8G21, 1948.

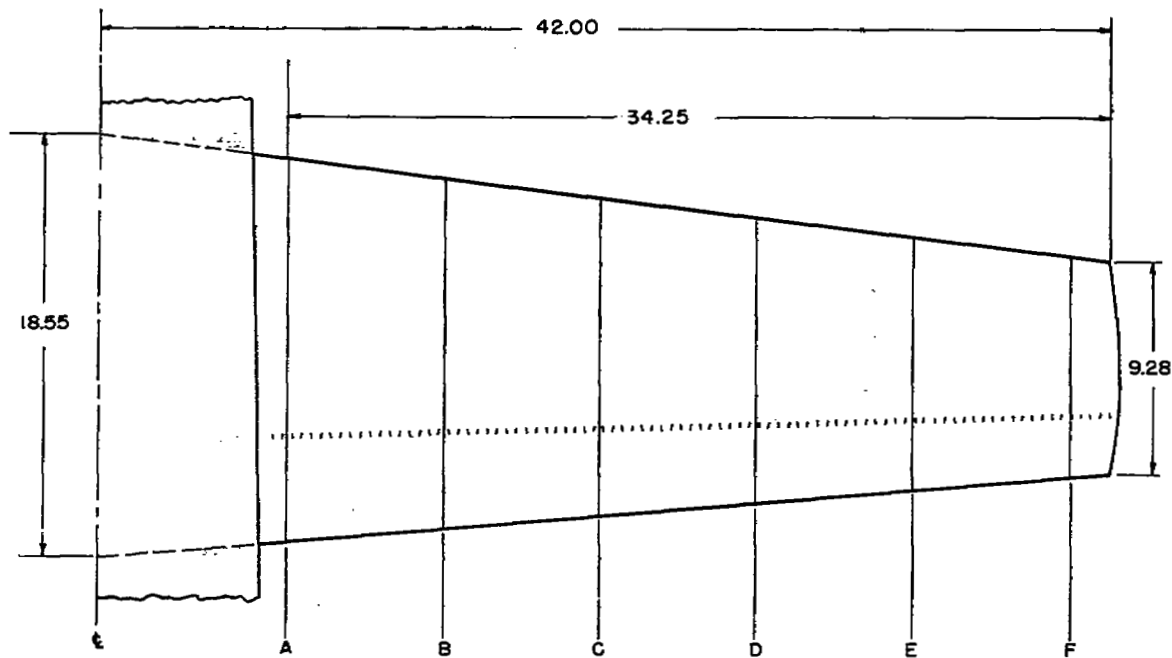
TABLE I.- SUMMARY OF SECTION AND WING PANEL NORMAL-FORCE  
COEFFICIENTS WITH VORTEX GENERATORS ON THE WING

M	$\alpha$ , deg	Section normal-force coefficient, $c_n$ , at station -						$C_N'$
		A	B	C	D	E	F	
$M \approx 0.69$								
0.689	-4.24	-0.184	-0.173	-0.172	-0.157	-0.115	-0.078	-0.151
.690	-1.96	.052	.070	.077	.084	.097	.044	.074
.690	0.32	.290	.315	.330	.333	.306	.175	.299
.689	2.62	.538	.576	.595	.598	.536	.330	.514
.691	4.87	.752	.800	.828	.828	.753	.502	.758
.690	5.99	.843	.886	.925	.924	.854	.597	.855
.689	6.64	.722	.861	.898	.912	.852	.614	.829
.690	6.98	.674	.846	.891	.914	.862	.628	.821
.689	7.89	.663	.822	.890	.920	.887	.669	.826
.690	8.86	.642	.799	.840	.828	.815	.654	.777
.690	9.86	.628	.783	.816	.813	.843	.678	.769
.690	10.86	.626	.788	.815	.788	.813	.686	.760
.691	11.87	.647	.806	.835	.825	.783	.691	.774
.691	12.92	.668	.830	.849	.792	.762	.693	.775
.689	14.98	.680	.713	.951	.887	.794	.754	.802
$M \approx 0.79$								
0.795	-4.36	-0.220	-0.218	-0.216	-0.198	-0.139	-0.095	-0.184
.789	-1.94	.067	.084	.096	.113	.120	.062	.093
.790	-1.94	.072	.097	.102	.120	.120	.065	.089
.791	0.44	.353	.386	.399	.413	.381	.224	.370
.793	0.45	.349	.382	.397	.409	.377	.222	.363
.793	2.79	.600	.639	.650	.662	.615	.393	.603
.792	3.91	.692	.735	.728	.732	.706	.475	.686
.793	4.99	.749	.786	.792	.802	.778	.551	.747
.794	6.06	.785	.789	.830	.837	.815	.607	.778
.791	7.10	.789	.810	.867	.879	.855	.660	.811
.793	8.05	.724	.809	.877	.906	.885	.702	.819
.793	9.06	.635	.790	.883	.920	.926	.748	.822
$M \approx 0.90$								
0.897	-4.37	-0.172	-0.195	-0.118	-0.163	-0.144	-0.084	-0.165
.898	-2.08	-.017	-.032	.015	-.047	0	.032	-.017
.897	0.20	.171	.159	.155	.132	.175	.148	.151
.897	2.57	.424	.419	.381	.409	.421	.309	.398
.898	4.88	.654	.639	.598	.636	.648	.464	.614
.899	6.97	.880	.854	.853	.885	.890	.614	.839
$M \approx 0.99$								
0.994	-4.42	-0.236	-0.244	-0.242	-0.225	-0.150	-0.070	-0.208
.993	-2.06	-.007	-.013	-.015	-.020	.019	.040	0
.995	0.35	.246	.250	.251	.233	.254	.156	.237
.993	2.74	.480	.487	.460	.436	.454	.280	.443
.992	4.93	.695	.707	.667	.665	.642	.406	.646



(a) Model dimensions.

Figure 1.- Sketch of 1/4-scale model of X-1 airplane (10-percent-thick wing) as tested in Langley 16-foot transonic tunnel. All dimensions in inches.



Spanwise locations of pressure measuring orifices

Span, station	A	B	C	D	E	F
Distance from model center line, percent semispan	18.5	33.8	49.1	64.4	79.8	95.1
Distance from station A, percent semispan	0	18.8	37.6	56.4	75.2	94.0

Chordwise locations of pressure measuring orifices (percent chord)

The distribution of orifices at all spanwise stations is identical.

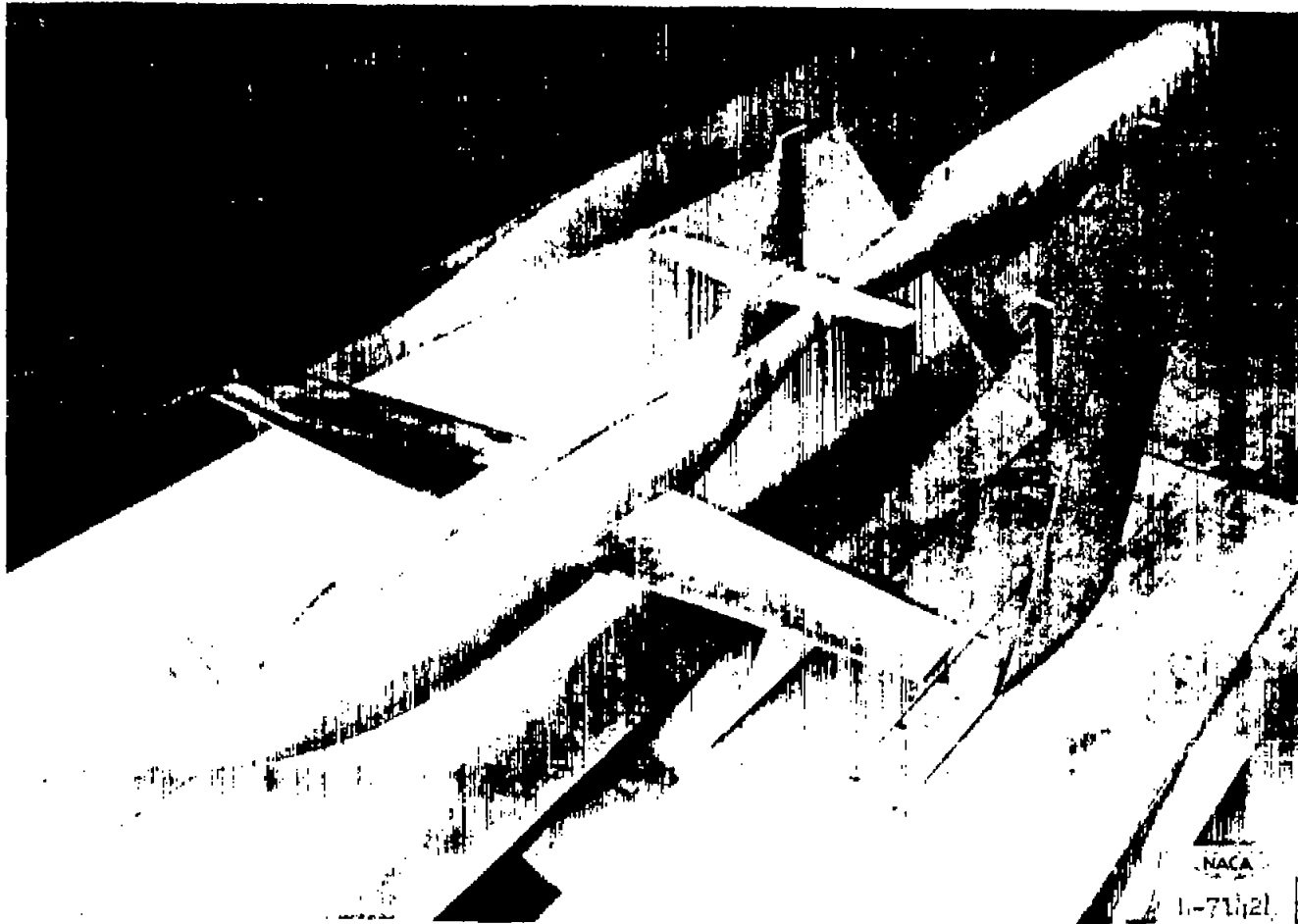
Upper surface 0, 1.25, 2.5, 5, 7.5, 10, 15, 20, 25, 30, 35, 40, 45, 50, 55, 60, 65, 70, 75, 80, 85, 90, 95  
 Lower surface 1.25, 2.5, 5, 7.5, 10, 15, 20, 25, 30, 35, 40, 45, 50, 55, 60, 65, 70, 75, 80, 85, 90, 95

Local wing station incidence

Span station	ε	A	B	C	D	E	F
Incidence, degrees	250	2.40	2.30	2.17	2.02	1.86	1.51

(b) Wing dimensions.

Figure 1.- Concluded.

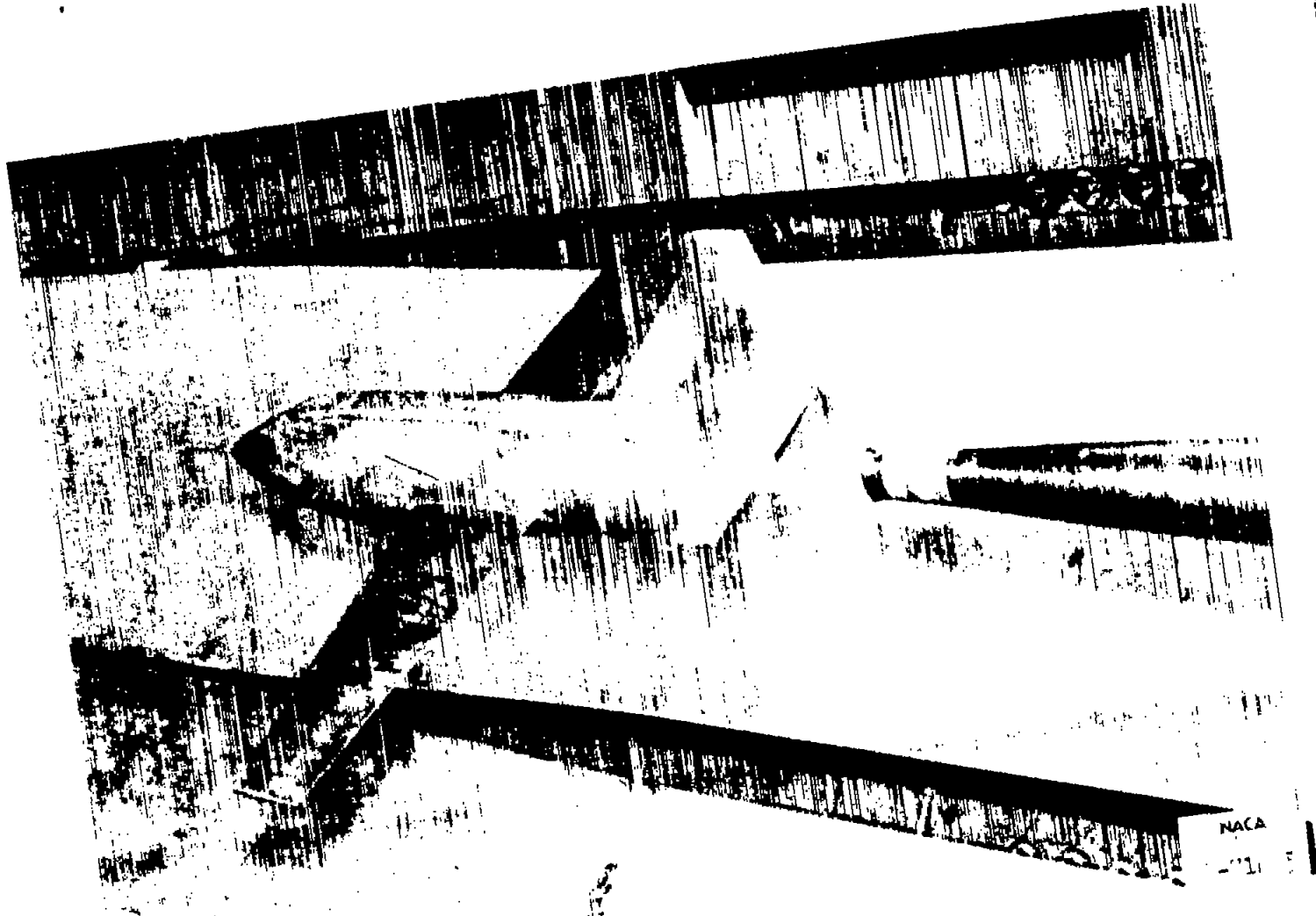


(a) Three-quarter front view.

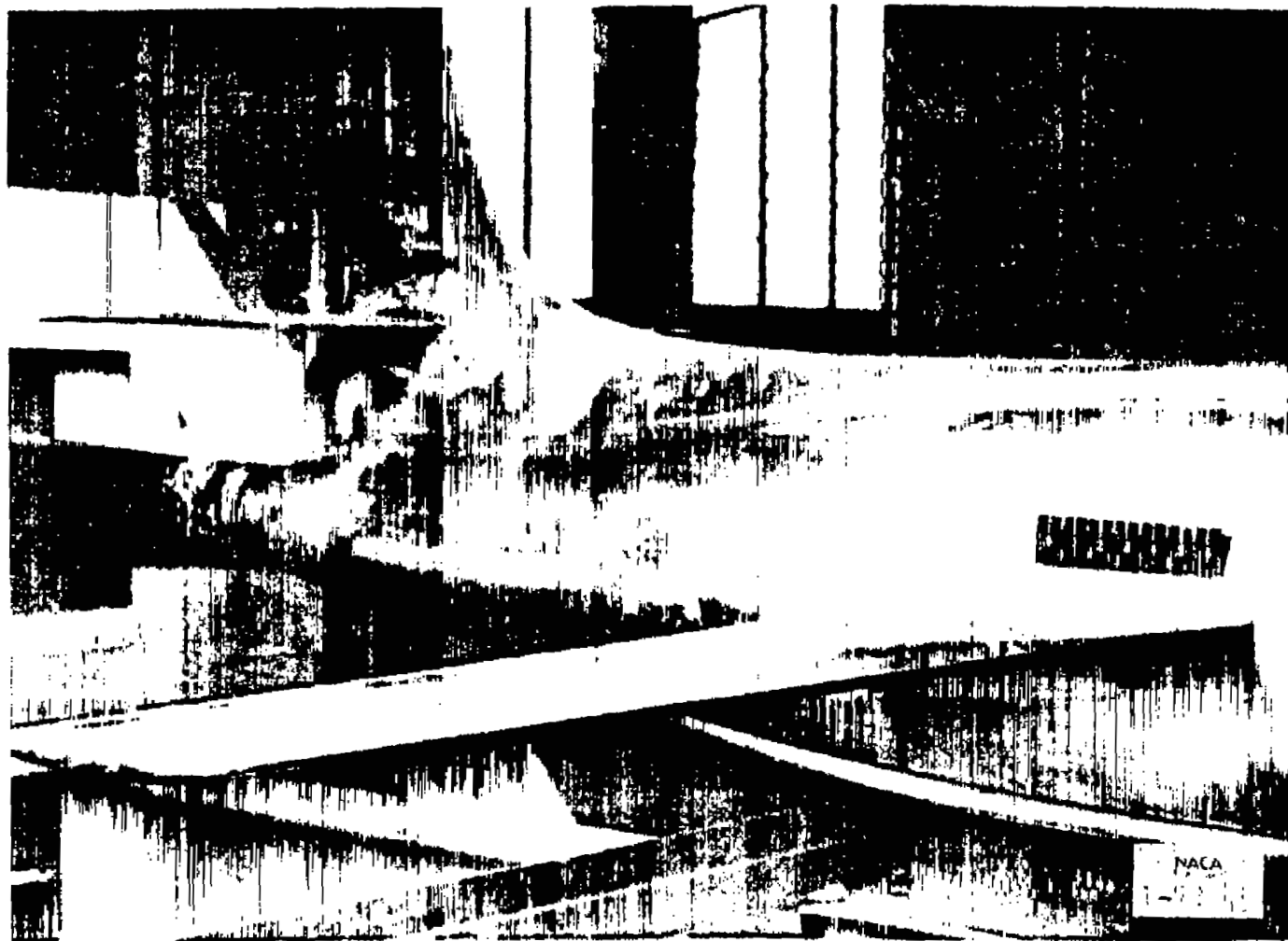
Figure 2.- Photograph of the 1/4-scale model of the X-1 airplane and model support system in the Langley 16-foot transonic tunnel.

4000

NACA RM 152126

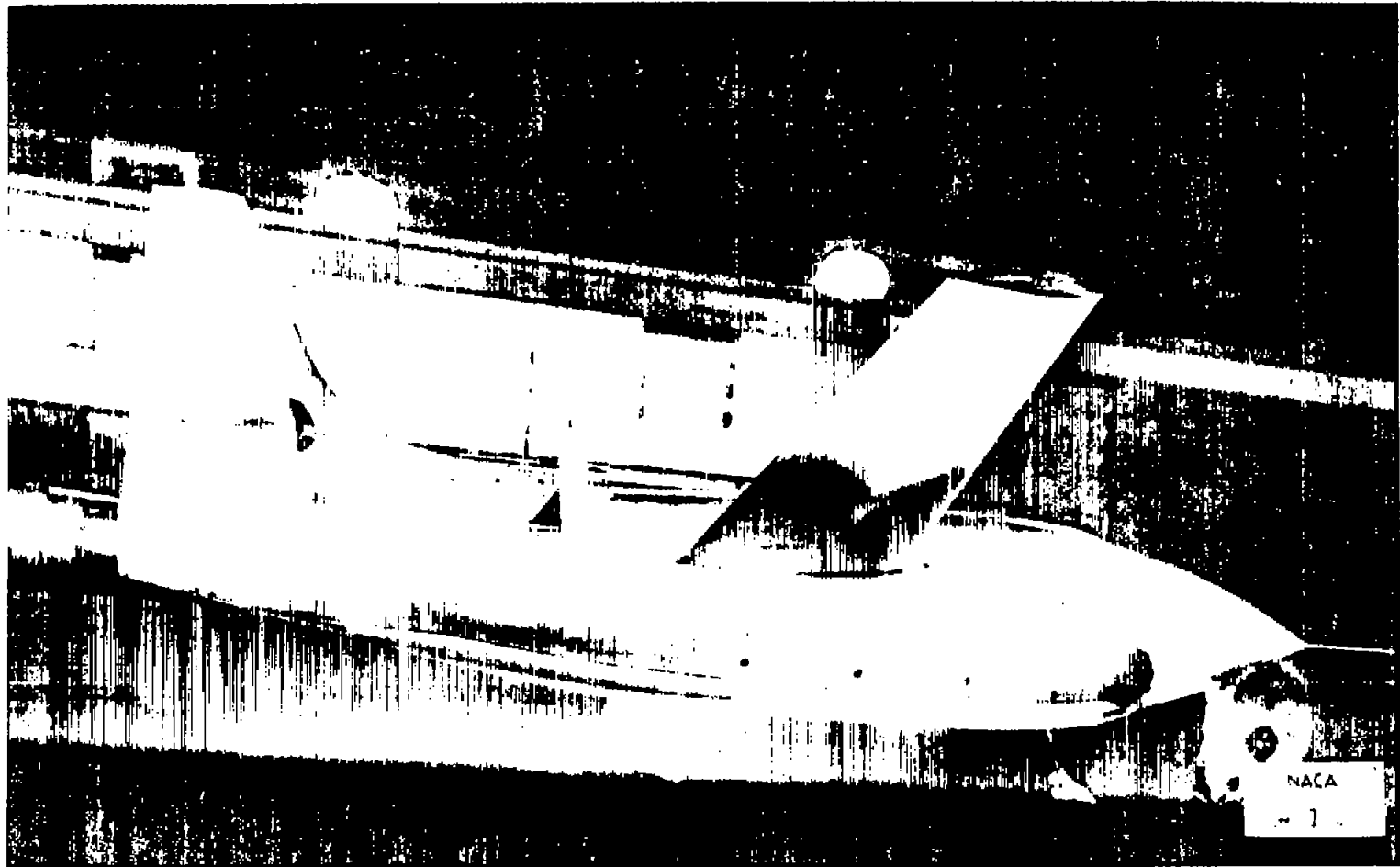


(b) Three-quarter rear view.  
Figure 2.- Concluded.



(a) 1/8-inch-square vortex-generator sections, full span.

Figure 3.- Details of model configurations.



(b) Wake-rake installation.

Figure 3.- Concluded.

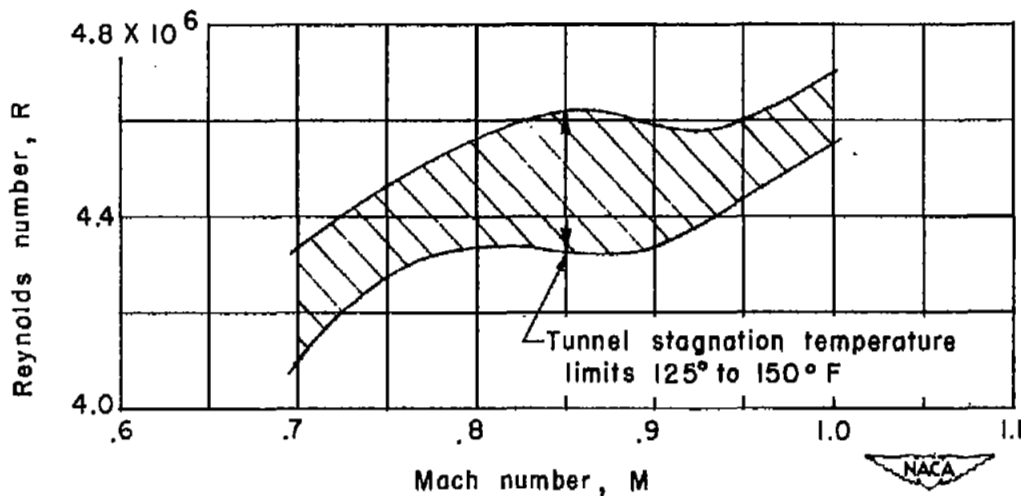
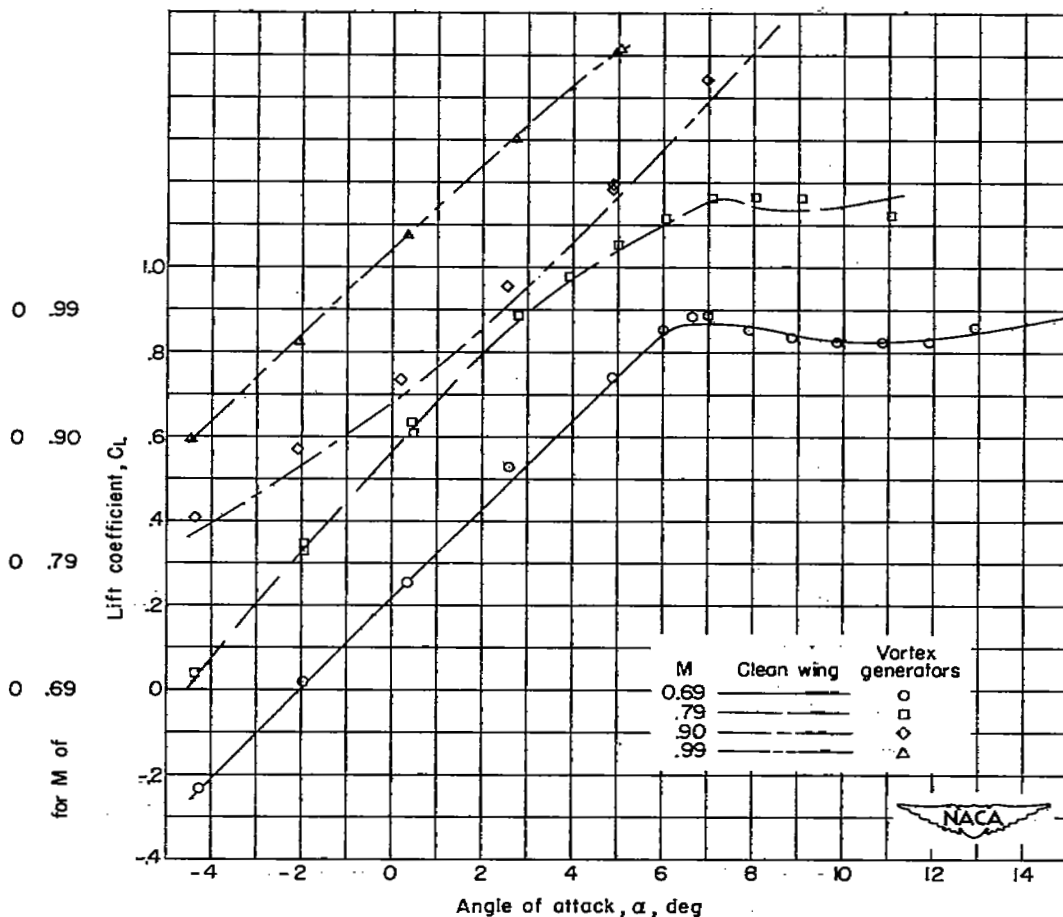
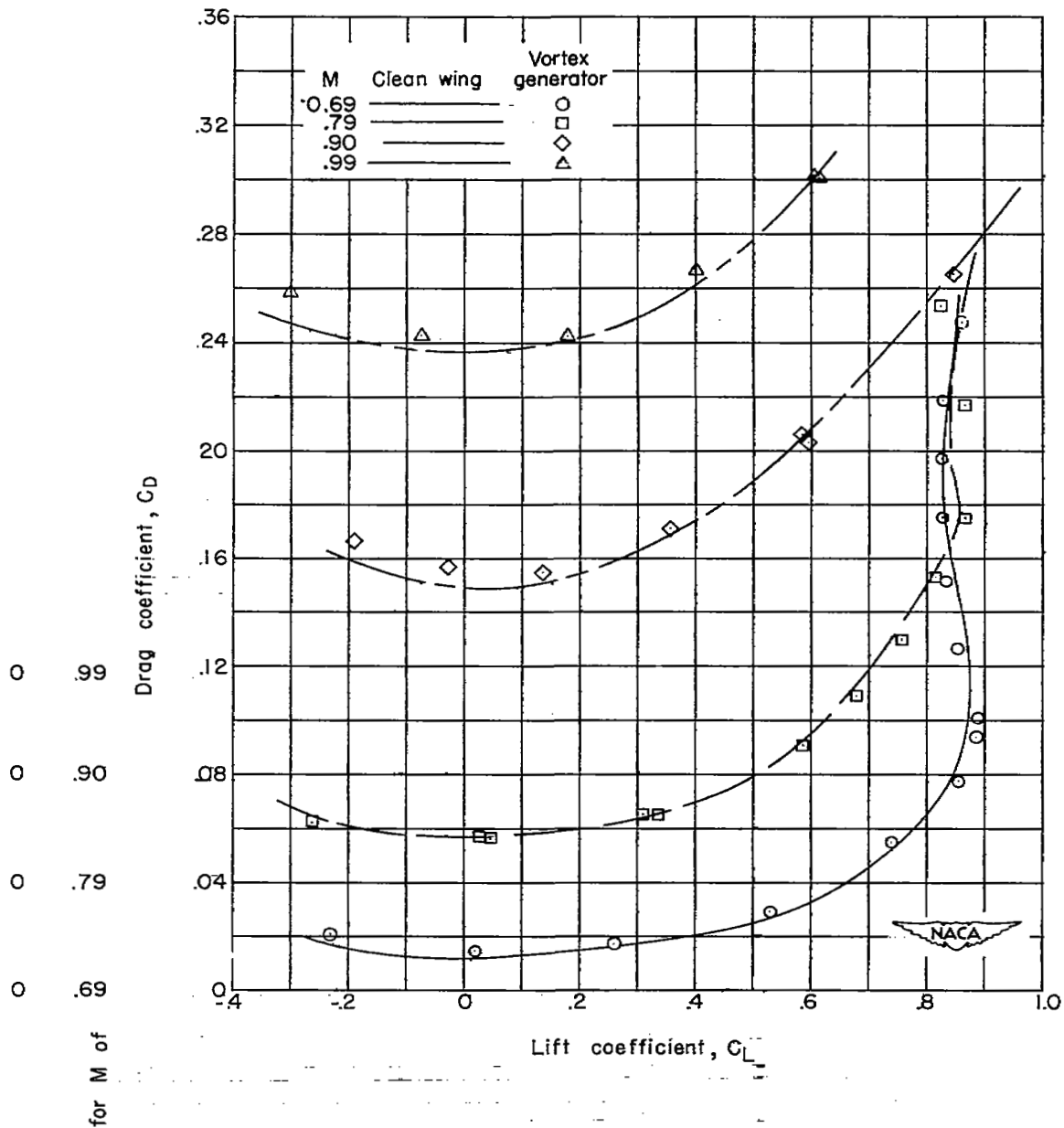


Figure 4.- Variation of Reynolds number with Mach number obtained in the investigation of a 1/4-scale model of the X-1 airplane in the Langley 16-foot transonic tunnel.  $c' = 1.203$  feet.



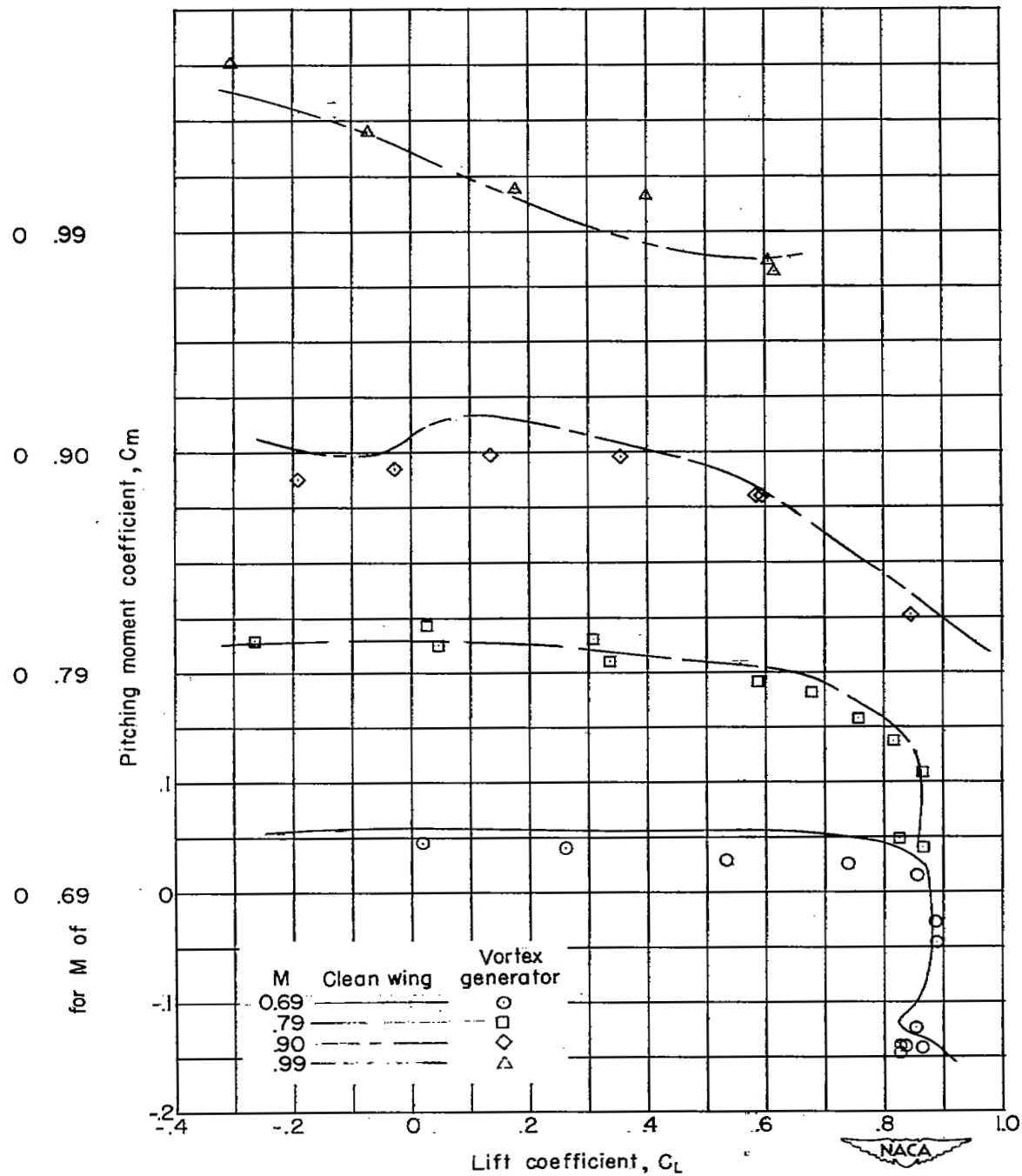
(a) Variation of lift coefficient with angle of attack.

Figure 5.- Aerodynamic characteristics of a 1/4-scale model of the X-1 airplane with vortex generators on the wing compared with clean wing.



(b) Variation of drag coefficient with lift coefficient.

Figure 5.- Continued.



(c) Variation of pitching-moment coefficient with lift coefficient.

Figure 5.- Concluded.

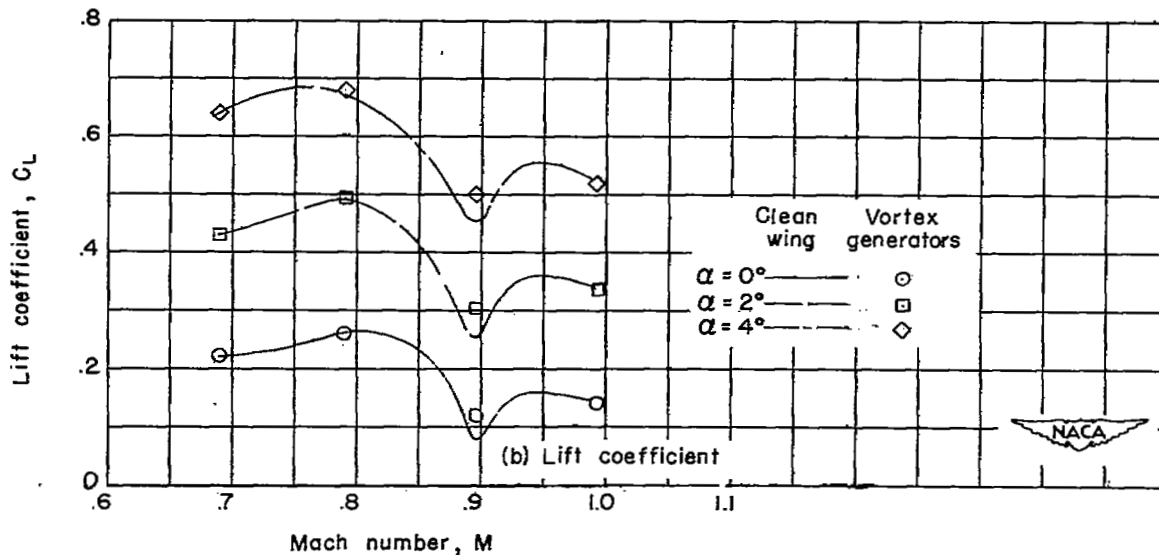
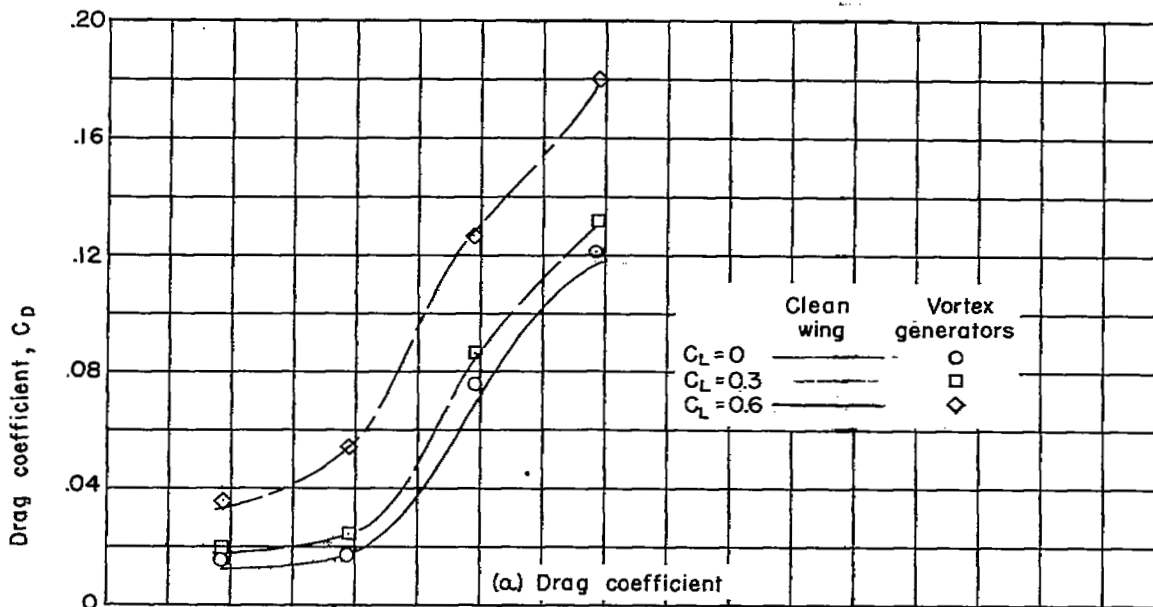
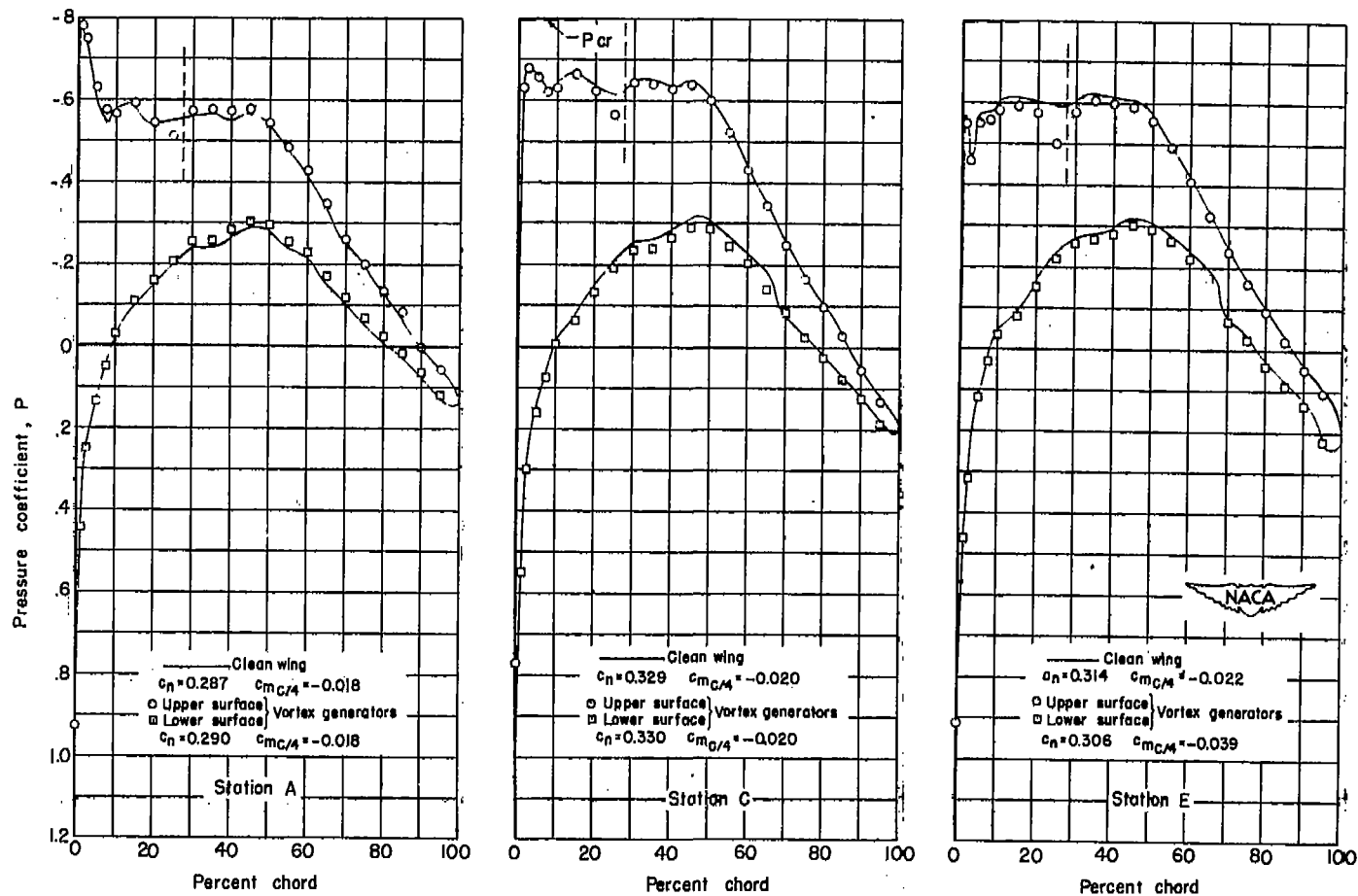
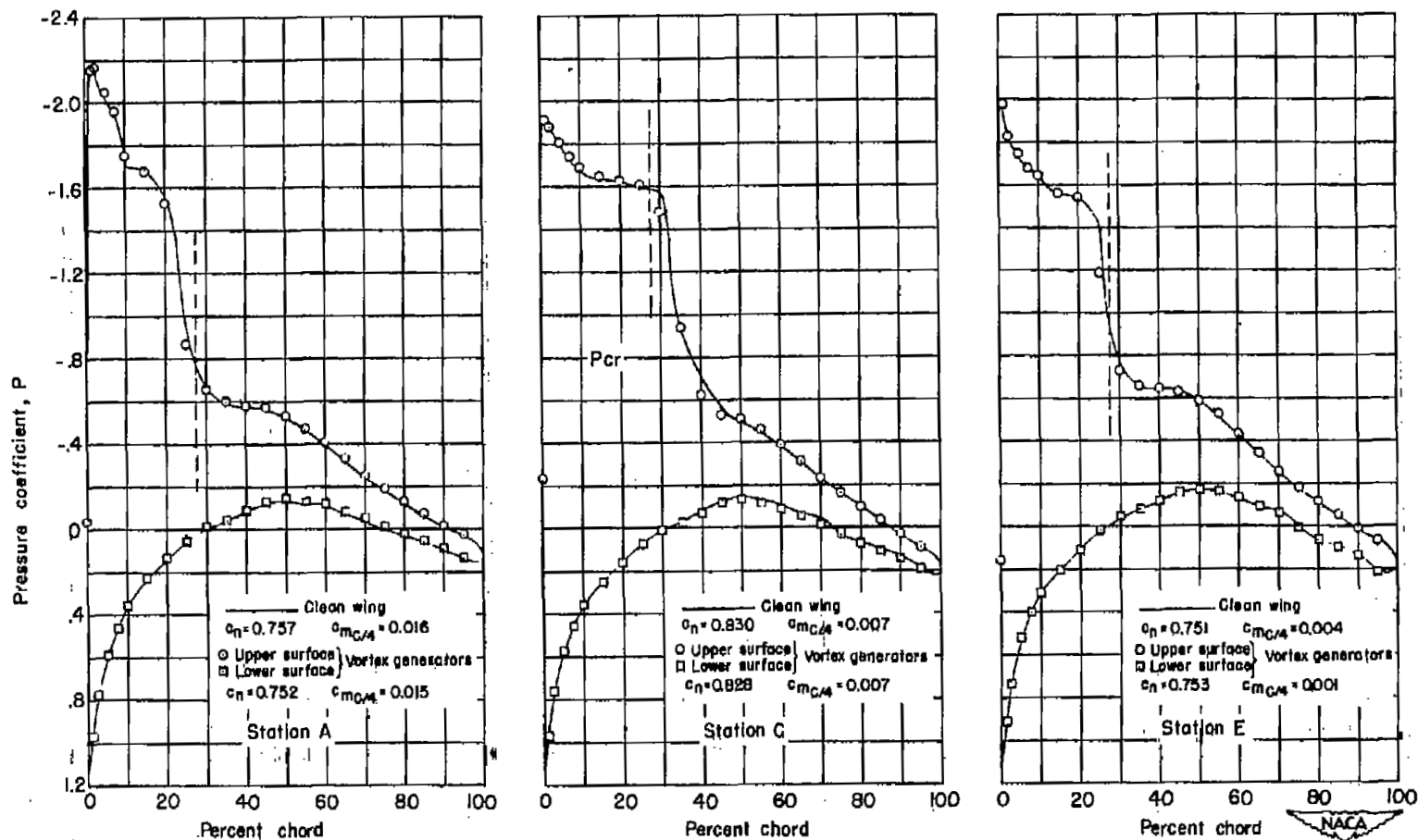


Figure 6.- Variation of aerodynamic characteristics with Mach number of 1/4-scale model of X-1 airplane with and without vortex generators on the wing.



(a) Clean wing;  $M = 0.689$ ;  $\alpha = 0.33^\circ$ . Vortex generators;  
 $M = 0.690$ ;  $\alpha = 0.32^\circ$ .

Figure 7.- Pressure distributions obtained on the clean wing of the 1/4-scale model of the X-1 airplane compared with pressure distributions obtained with vortex generators on the wing at  $M = 0.69$ .



(b) Clean wing;  $M = 0.692$ ;  $\alpha = 4.81^\circ$ . Vortex generators;  
 $M = 0.691$ ;  $\alpha = 4.87^\circ$ .

Figure 7.- Concluded.

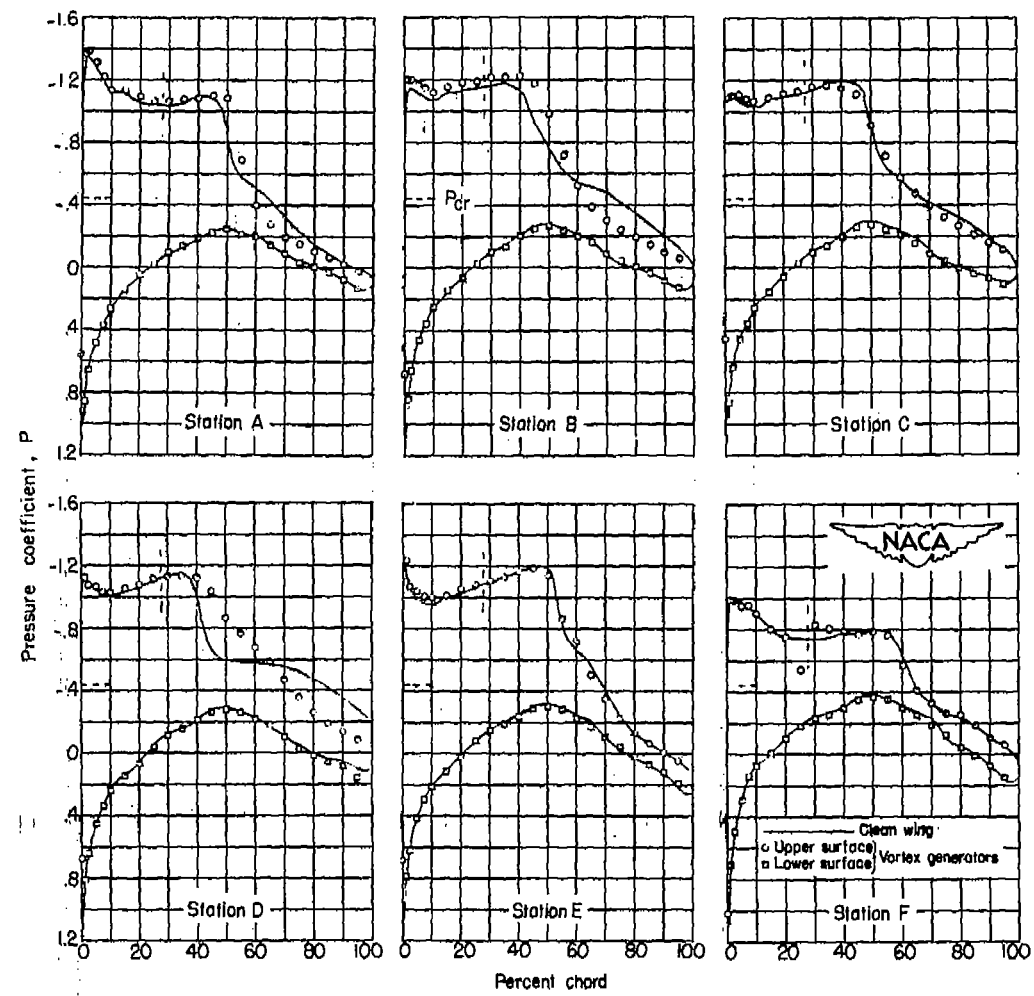
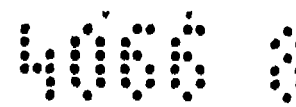
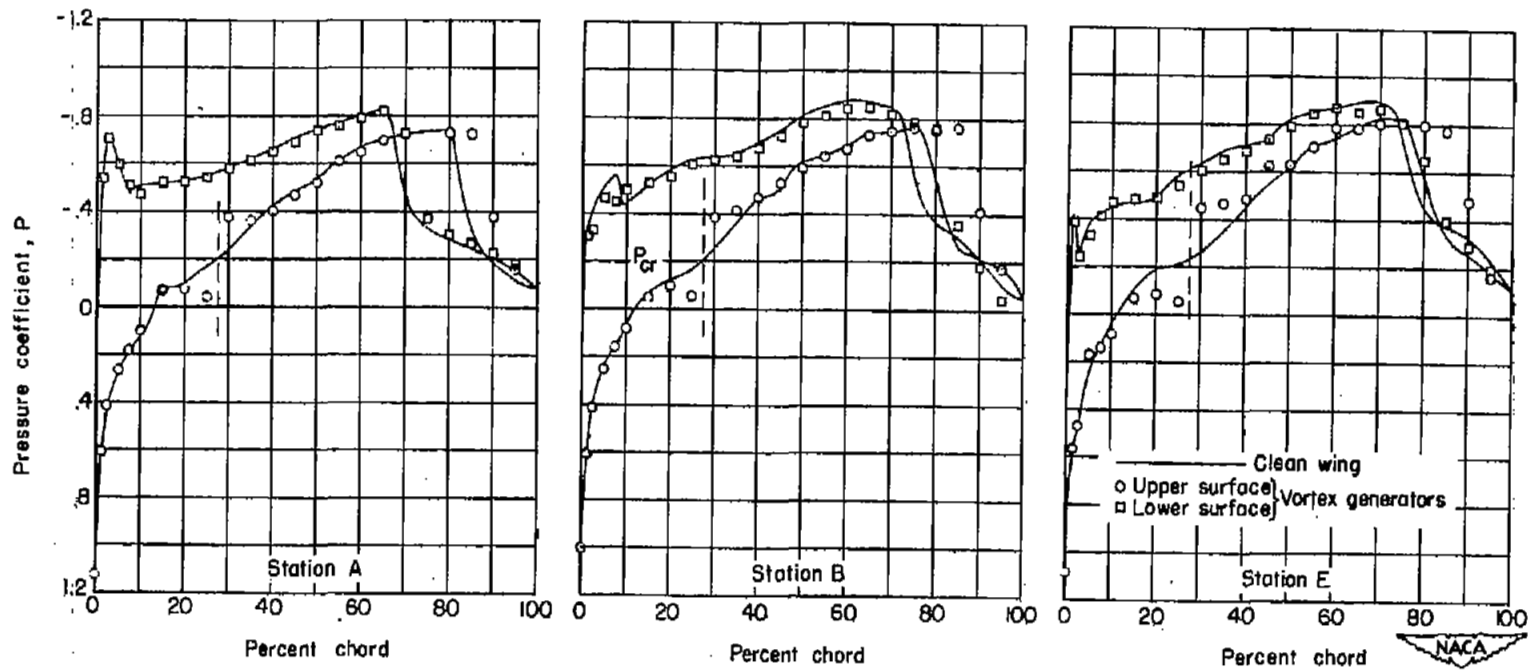
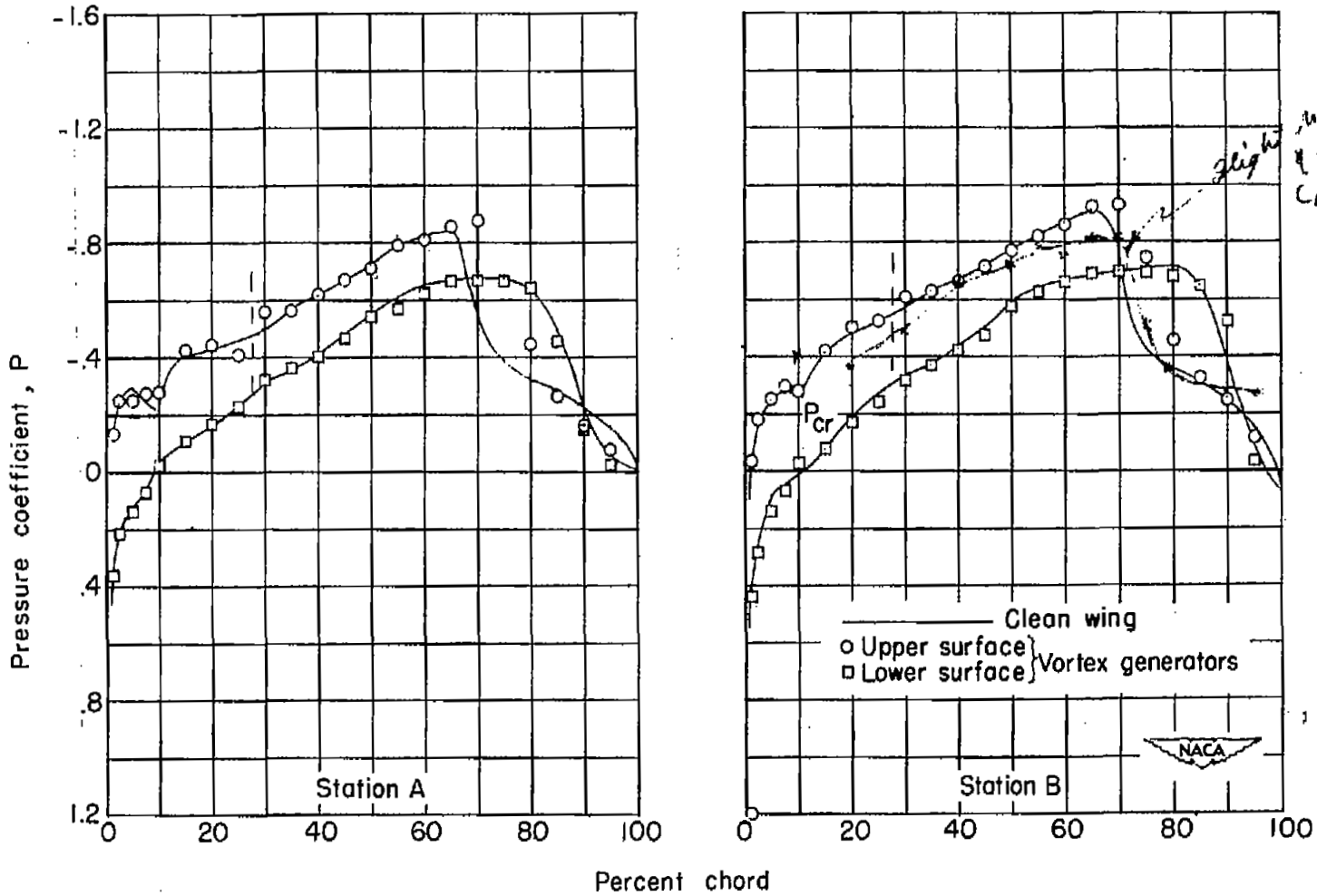


Figure 8.- Pressure distributions obtained on clean wing of a 1/4-scale model of the X-1 airplane compared with pressure distributions obtained with vortex generators on the wing. Clean wing;  $M = 0.799$ ;  $\alpha = 3.92^\circ$ . Vortex generators;  $M = 0.792$ ;  $\alpha = 3.91^\circ$ .



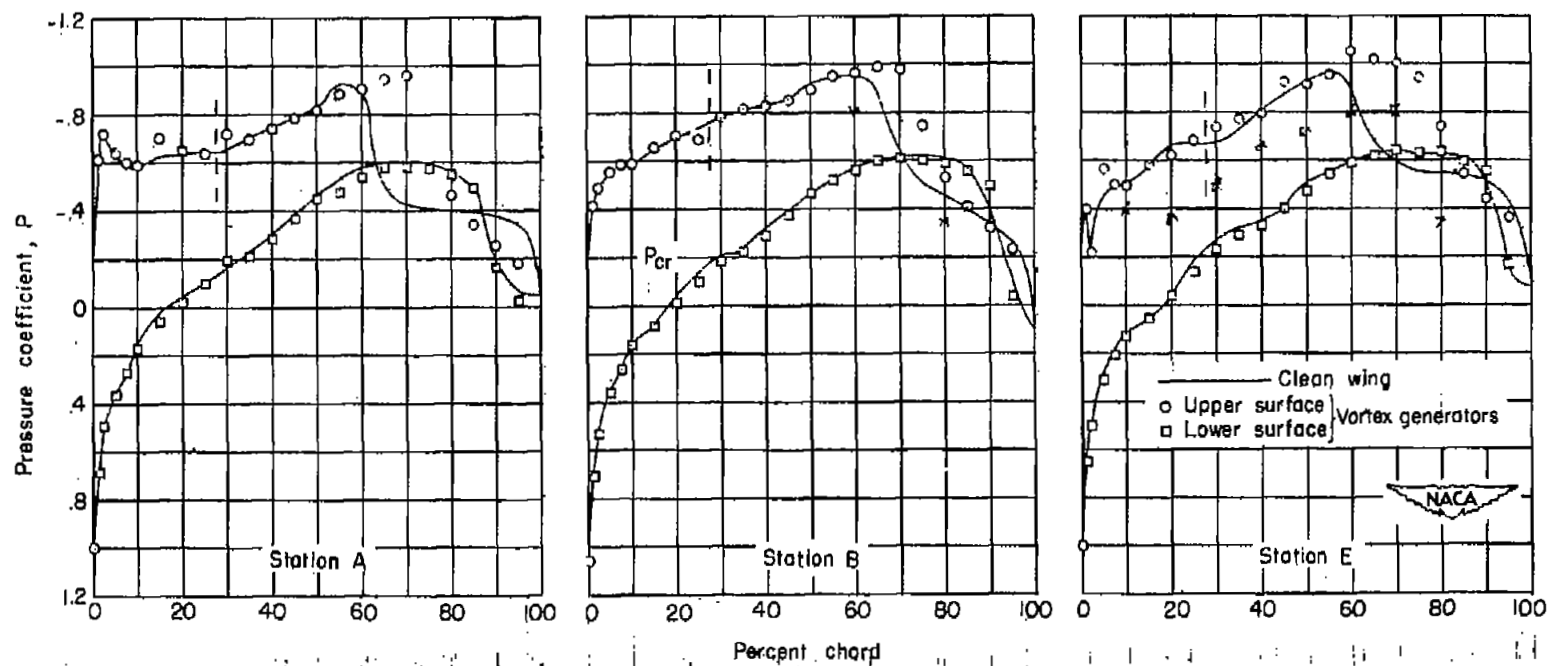
(a) Clean wing;  $M = 0.893$ ;  $\alpha = -4.38^\circ$ . Vortex generators;  
 $M = 0.897$ ;  $\alpha = -4.37^\circ$ .

Figure 9.- Pressure distributions obtained on clean wing of the 1/4-scale model of the X-1 airplane compared with pressure distributions obtained with vortex generators on the wing at  $M \approx 0.90$ .



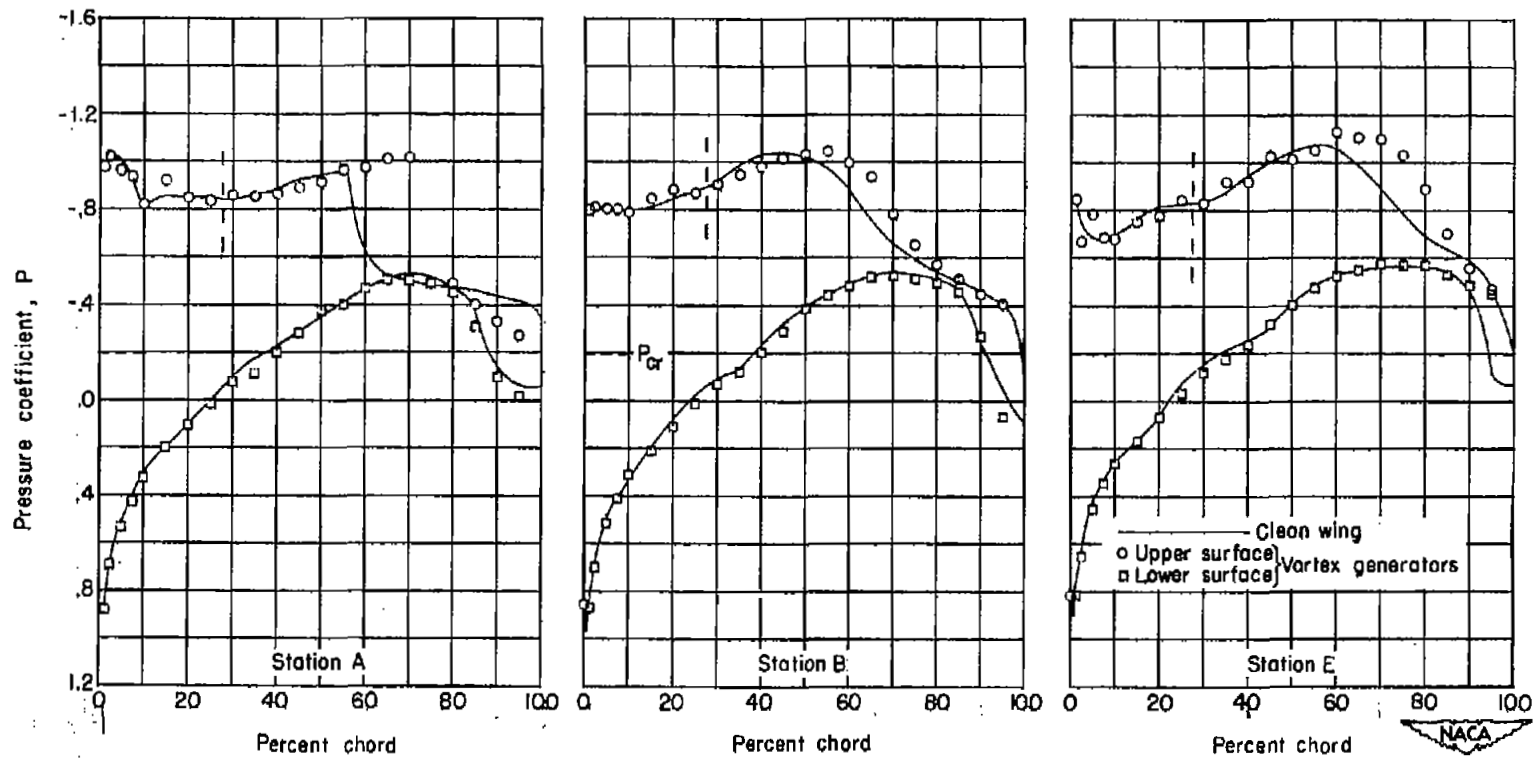
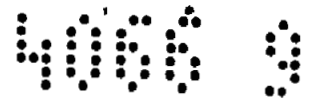
(b) Clean wing;  $M = 0.894$ ;  $\alpha = 0.17^\circ$ . Vortex generators;  
 $M = 0.897$ ;  $\alpha = 0.20^\circ$ .

Figure 9.- Continued.



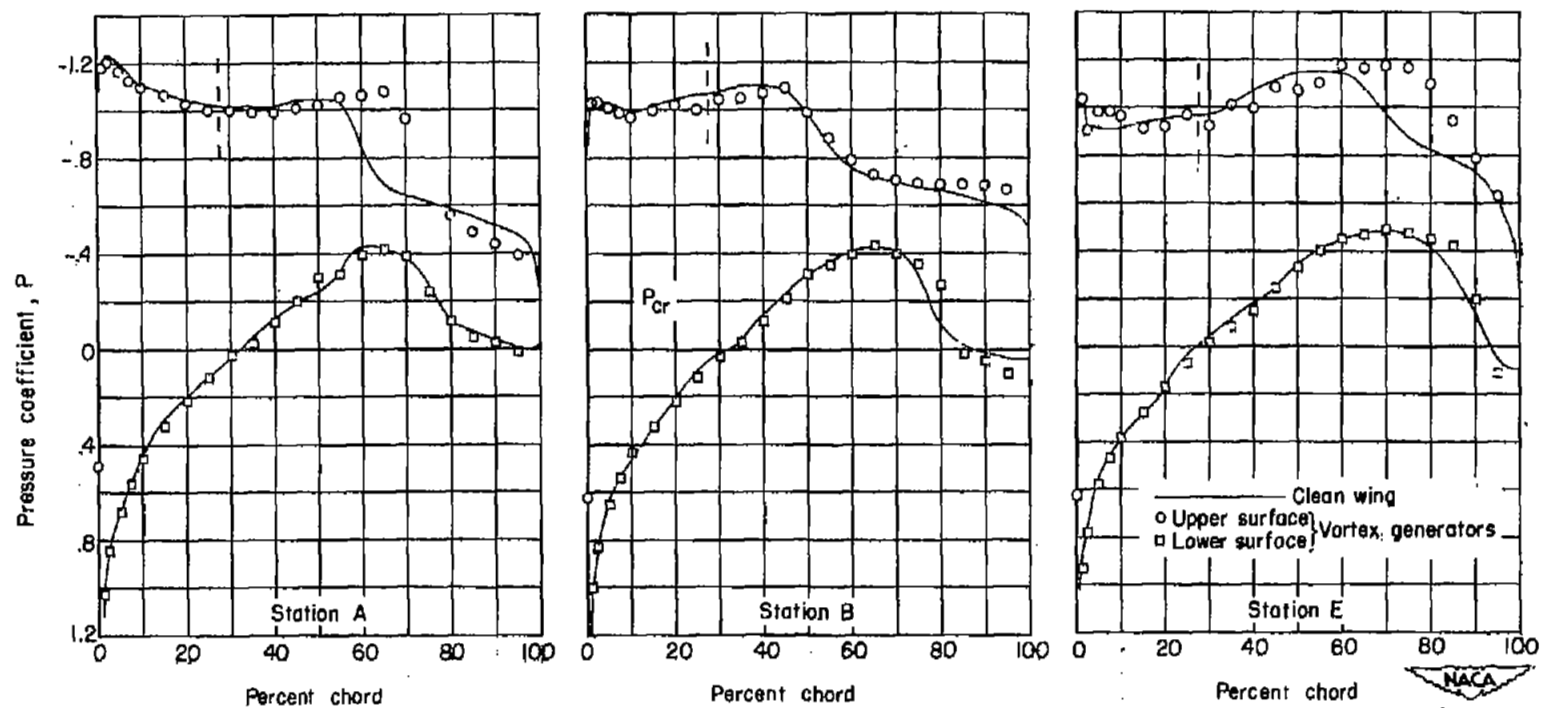
(c) Clean wing;  $M = 0.893$ ;  $\alpha = 2.57^\circ$ . Vortex generators;  
 $M = 0.897$ ;  $\alpha = 2.57^\circ$ .

Figure 9.- Continued.



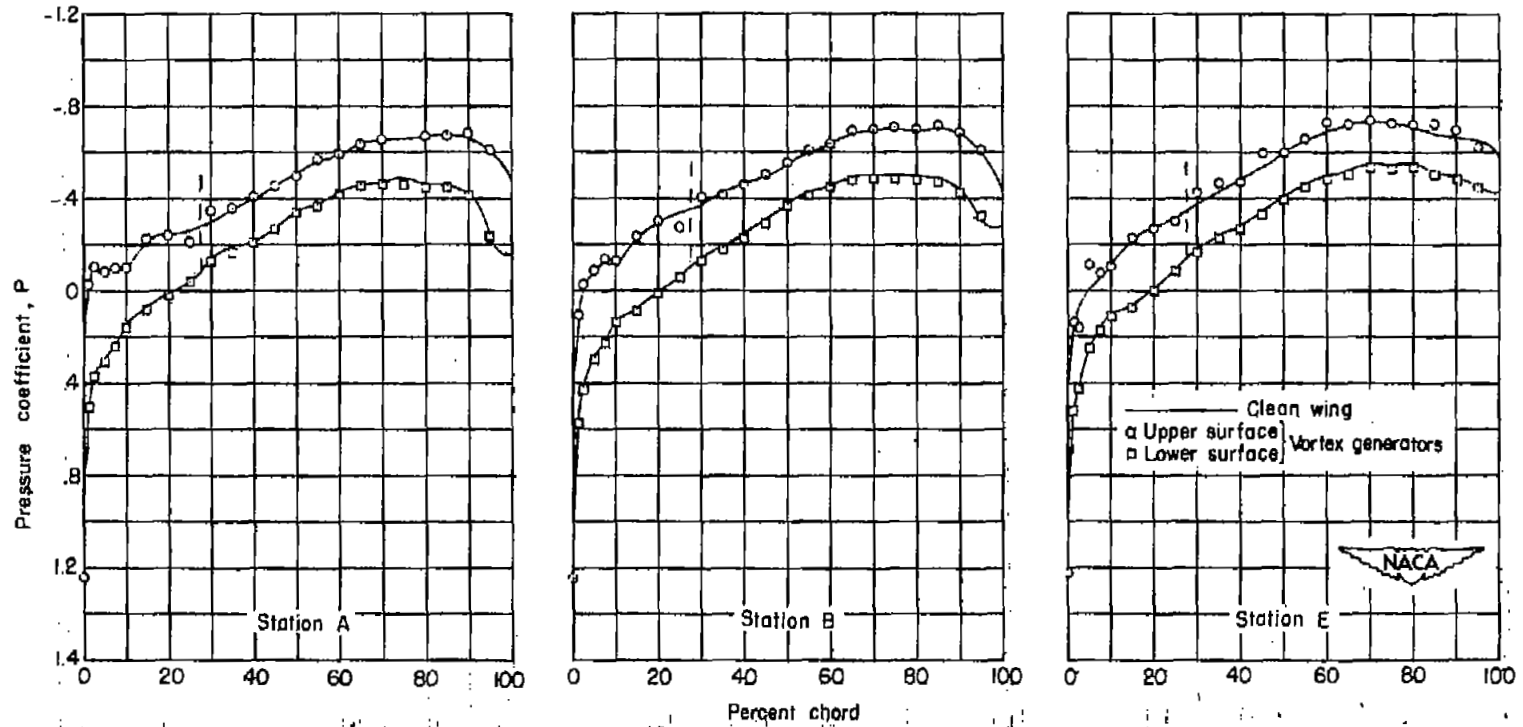
(d) Clean wing;  $M = 0.894$ ;  $\alpha = 4.84^\circ$ . Vortex generators;  
 $M = 0.898$ ;  $\alpha = 4.88^\circ$ .

Figure 9.- Continued.



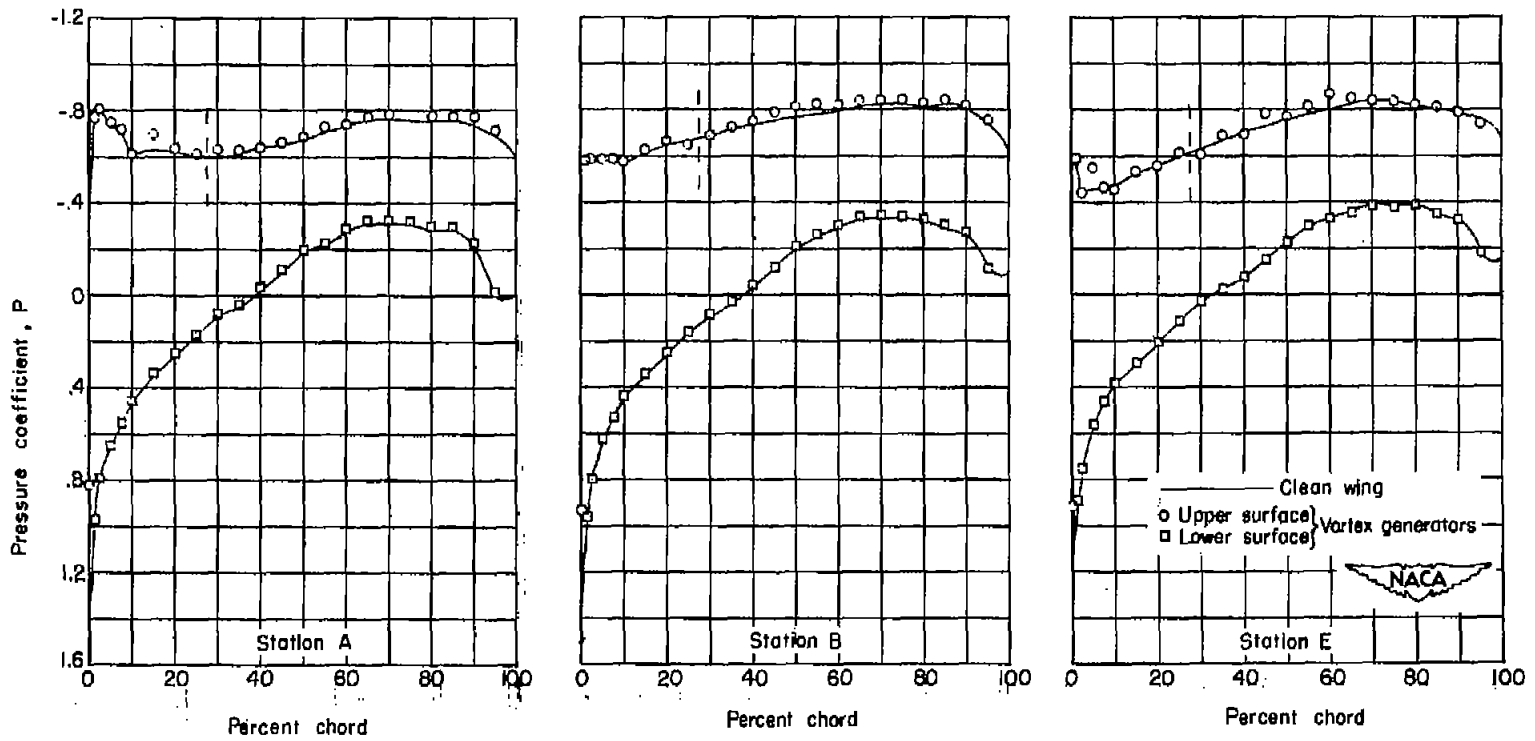
(e) Clean wing;  $M = 0.892$ ;  $\alpha = 7.21^\circ$ . Vortex generators;  
 $M = 0.899$ ;  $\alpha = 6.97^\circ$ .

Figure 9.- Concluded.



(a). Clean wing;  $M = 0.991$ ;  $\alpha = 0.33^\circ$ . Vortex generators;  
 $M = 0.995$ ;  $\alpha = 0.35^\circ$ .

Figure 10.- Pressure distributions obtained on clean wing of the 1/4-scale model of the X-1 airplane compared with pressure distributions obtained with vortex generators on the wing at  $M = 0.99$ .



(b) Clean wing;  $M = 0.998$ ;  $\alpha = 5.15^\circ$ . Vortex generators;  
 $M = 0.992$ ;  $\alpha = 4.93^\circ$ .

Figure 10.- Concluded.

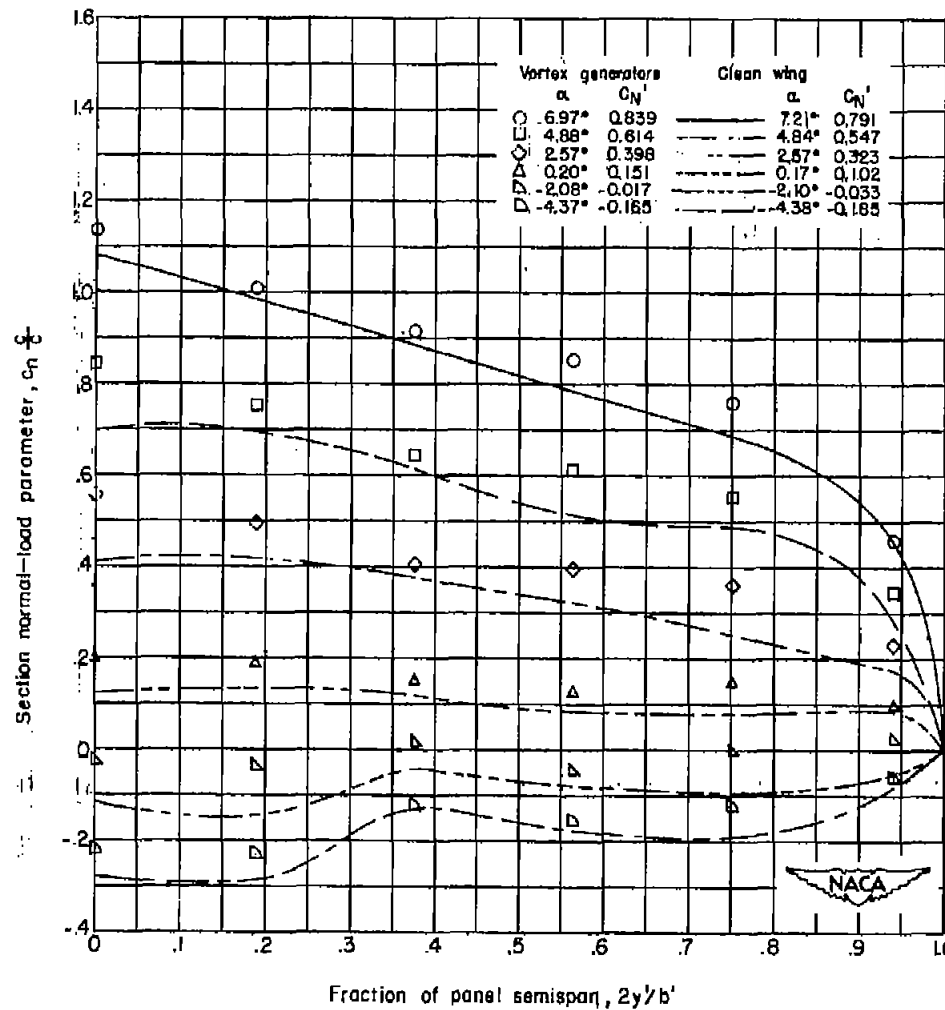
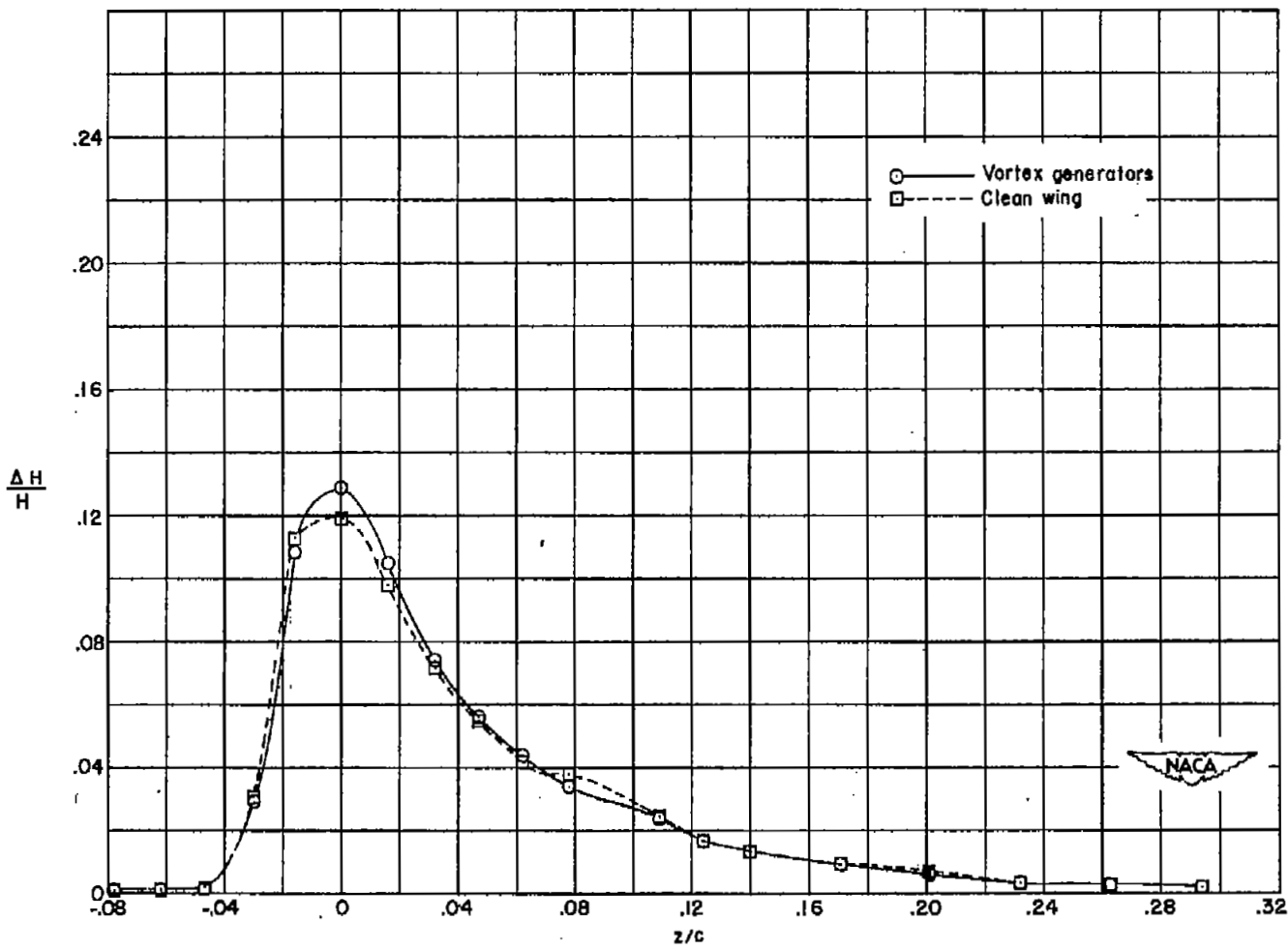
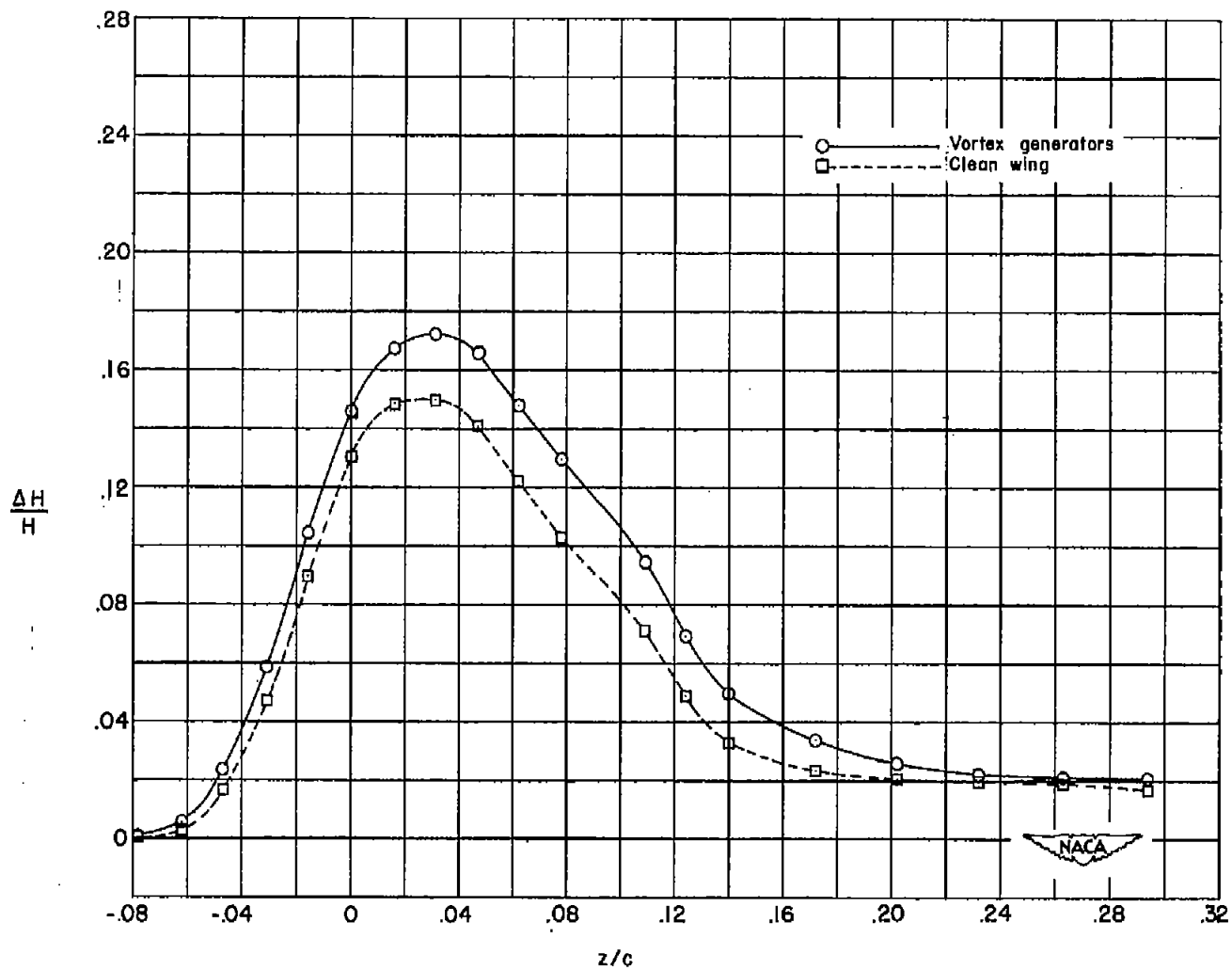


Figure 11.- Spanwise loading distributions obtained on clean wing of the X-1 airplane compared with spanwise loading distributions obtained with vortex generators on the wing at  $M \approx 0.90$  for several angles of attack.



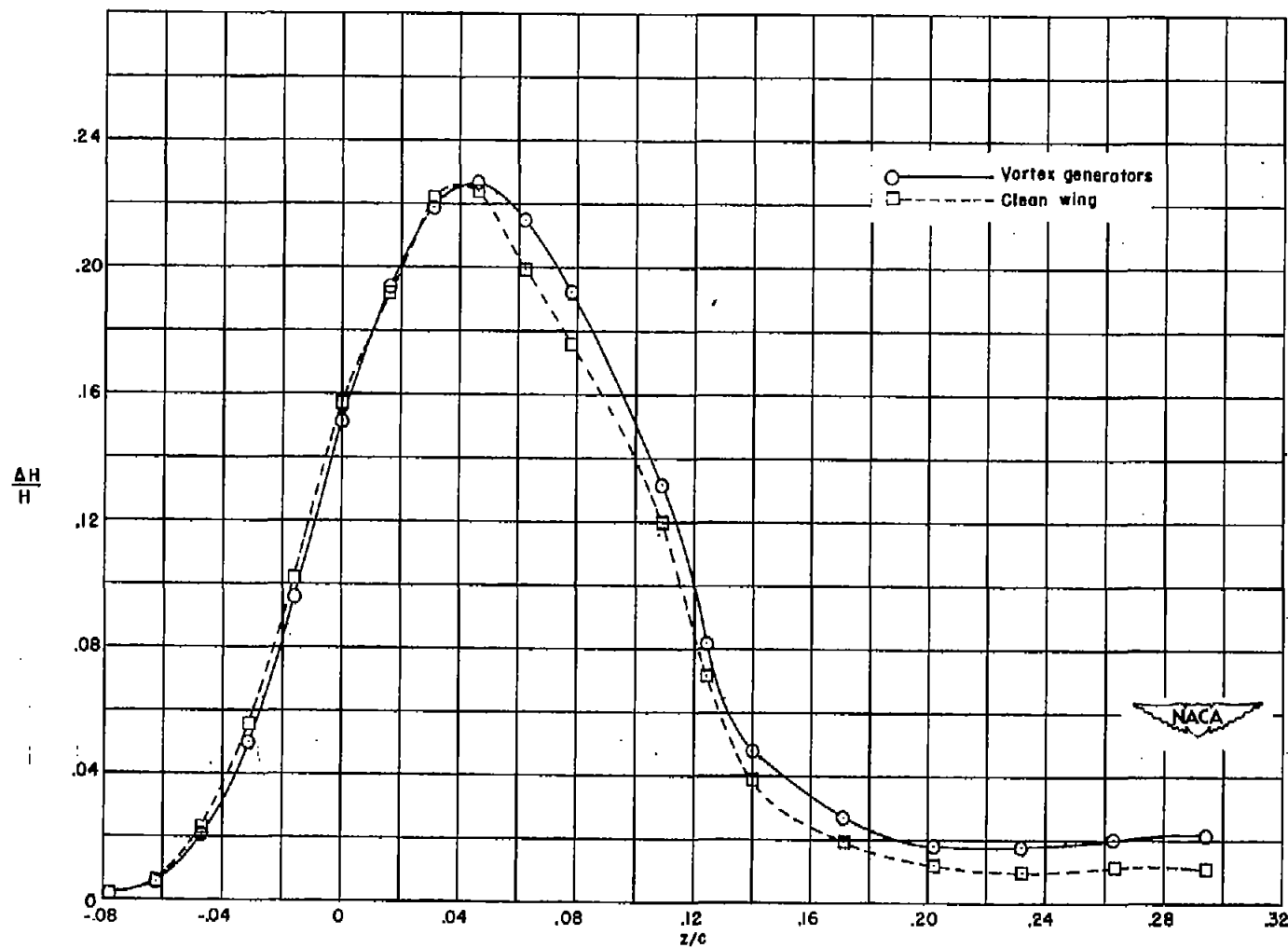
(a)  $M = 0.70; \alpha \approx 4.8^\circ$ .

Figure 12.- Wake patterns obtained from configurations having clean wing and wing with vortex generators installed.



(b)  $M = 0.80$ ;  $\alpha = 4.9^\circ$ .

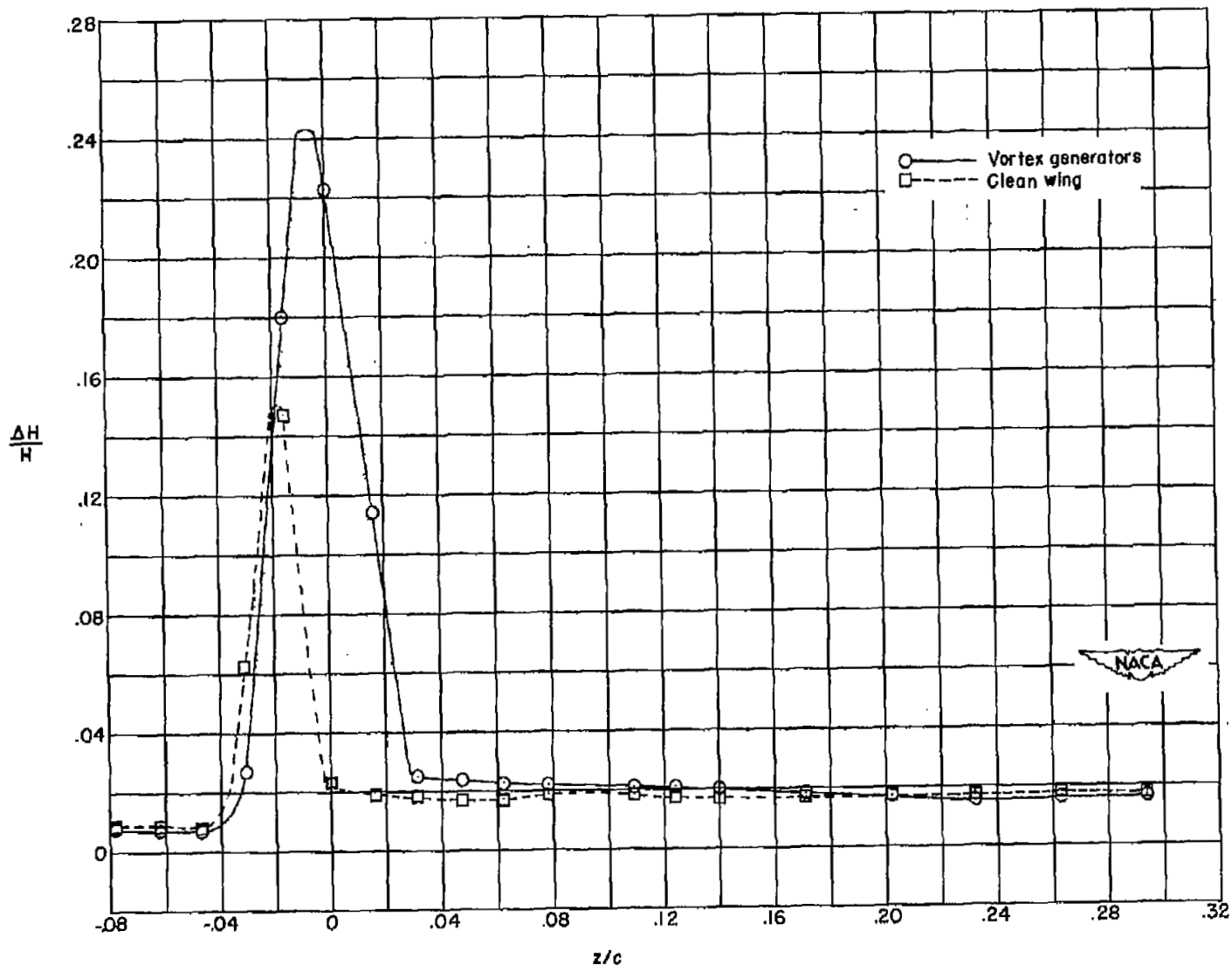
Figure 12.- Continued.



(c)  $M = 0.85; \alpha \approx 4.9^\circ$ .

Figure 12.- Continued.





(d)  $M = 1.00$ ;  $\alpha \approx 0.3^\circ$ .

Figure 12.- Concluded.

UNCLASSIFIED

NACA RM L52L26

~~CONFIDENTIAL~~

INDEX

<u>Subject</u>	<u>Number</u>
Boundary-Layer - Wing Sections	1.2.1.6
Mach Number Effects - Wing Sections	1.2.1.8
Wing Sections - Wake	1.2.1.9
Airplanes - Specific Types	1.7.1.2
Loads, Aerodynamic - Wings	4.1.1.1

ABSTRACT

An investigation of a vortex-generator configuration on the wings of a 1/4-scale model of the X-1 airplane showed a reduction in separation due to shock at a Mach number of 0.90. The vortex generators were relatively ineffective at other speeds.

UNCLASSIFIED

~~CONFIDENTIAL~~